

https://doi.org/10.1093/plcell/koaf196 Advance access publication 8 August 2025 Research Article

Photoexcited CRY1 physically interacts with ATG8 to regulate selective autophagy of HY5 and photomorphogenesis in *Arabidopsis*

Lu Jiang, ^{1,2,†} Shilong Zhang, ^{1,2,†} Yuting Niu, ^{1,2} Guangqiong Yang, ^{1,2} Jiachen Zhao, ^{1,2} Huishan Liu, ^{1,2} Minyu Xiong, ^{1,2} Lingyi Xie, ^{1,2} Zhilei Mao, ^{1,2} Tongtong Guo, ^{1,2} Hong-Quan Yang, ^{1,2,*} Wenxiu Wang, ^{1,2,*}

Abstract

Cryptochromes (CRYs) are blue light photoreceptors that regulate various light responses in plants, including photomorphogenesis. Autophagy is a tightly controlled intracellular degradation pathway that plays a critical role in plant growth and development. CRY signaling inhibits the 26S proteasome-dependent degradation of LONG HYPOCOTYL 5 (HYS) through interactions with the CONSTITUTIVE PHOTOMORPHOGENIC1 (COP1)–SUPPRESSOR OF PHYA-105 1 (SPA1) complex. However, whether CRY1 mediates the blue light-driven regulation of photomorphogenesis by regulating the autophagic degradation of HY5 remains unclear. Here, we show that CRY1 directly interacts with ATG8, a key player in selective autophagy, in a blue light-dependent manner in Arabidopsis (Arabidopsis haliana). ATG8 and ATG5/ATG7 act genetically downstream of CRY1, but upstream of HY5, to regulate photomorphogenesis. In darkness, AUTOPHAGY-RELATED8 (ATG8) physically interacts with HY5 to facilitate its autophagic degradation and promote skotomorphogenesis. Under blue light, the CRY1–ATG8 interaction inhibits the ATG8–HY5 interaction, suppressing the nuclear export and co-localization of ATG8 and HY5 to the autophagosome, and HY5 degradation in the vacuole. This study reveals how CRY1-mediated blue light signaling regulates HY5 autophagy, which enables plants to fine-tune photomorphogenic development in response to light and nutrient availability.

Introduction

Light serves as a crucial environmental signal, providing energy and regulating various developmental processes throughout a plant's lifecycle (Deng and Quail 1999). To sense light, plants have evolved diverse photoreceptors that monitor both quantitative and qualitative changes in light. These include blue/UV-A light receptors cryptochromes (CRY1 and CRY2, CRYs), phototropins (PHOT1 and PHOT2), red/far-red light receptors (phytochromes: phyA-phyE), and the UV-B receptor UVR8 (Ahmad and Cashmore 1993; Briggs and Christie 2002; Quail 2002; Rizzini et al. 2011). Among these, CRYs are the only photoreceptors conserved across all major evolutionary lineages, underscoring their fundamental role. CRYs mediate key physiological processes in plants, including photomorphogenesis, photoperiodic flowering, circadian rhythm regulation, stomatal function, and DNA repair (Ahmad and Cashmore 1993; Guo et al. 1998, 2023; Somers et al. 1998; Briggs and Christie 2002; Ohgishi et al. 2004; Mao et al. 2005; Liu et al. 2008; Kang et al. 2009; Cao et al. 2021; Wang et al. 2021b). Skotomorphogenesis is characterized by elongated hypocotyls and folded and closed cotyledons, which enable them to penetrate the soil and capture the sunlight. Photomorphogenesis is notably characterized by reduced elongation of hypocotyls, unfolded and expanded cotyledons, and chlorophyll accumulation, which allows them to carry out photosynthesis and begin autotrophic growth. Recent studies have also revealed a noncanonical role of CRY2 in darkness, where it modulates the Arabidopsis transcriptome and suppresses cell division in the root apical meristem, leading to reduced root elongation (Zeng et al. 2025). CRYs regulate the circadian clock in *Drosophila melanogaster* and *Mammalia* (Emery et al. 1998; Kume et al. 1999) and enable migratory birds to sense the Earth's magnetic field for navigation (Gegear et al. 2010).

CRYs structurally consist of an N-terminal photolyase homologous region (PHR) domain and a C-terminal extension (CCE) (Yang et al. 2000; Yu et al. 2010). The PHR domain supports homodimerization of CRY1 and CRY2 (Sang et al. 2005; Yu et al. 2007), a process essential for photoreceptor activity but inhibited by Blue light Inhibitors of Cryptochromes 1 (BIC1) (Wang et al. 2016). This domain also facilitates interactions with key transcription regulators in phytohormone signaling, such as Aux/IAA, AUXIN RESPONSE FACTOR (ARF) (for auxin), BRI1-EMS-SUPPRESSOR 1 (BES1) (for BR), and DELLA proteins, to coordinate photomorphogenesis (Wang et al. 2018; Xu et al. 2018, 2021; Mao et al. 2020; Zhong et al. 2021). Additionally, the PHR domain mediates blue light-dependent interactions with proteins like PHYTOCHROME INTERACTING FACTORS (PIFs), ARABIDOPSIS G-PROTEIN BETA 1 (AGB1), SWR1 Complex Subunit 6 (SWC6)/Actin-Related Protein 6 (ARP6), and Structural Maintenance of Chromosomes 5 (SMC5)/Alteration/Deficiency in Activation 2B (Ada2b), which regulate photomorphogenesis and DNA repair (Ma et al. 2016;

¹Shanghai Key Laboratory of Plant Molecular Sciences, College of Life Sciences, Shanghai Normal University, Shanghai 200234, China

²Shanghai Collaborative Innovation Center of Plant Germplasm Resources Development, College of Life Sciences, Shanghai Normal University, Shanghai 200234, China

^{*}Author for correspondence: hqyang@shnu.edu.cn (H.-Q.Y.), wangwenxiu85@shnu.edu.cn (W.W.)

[†]These authors contributed equally to this work.

The author responsible for distribution of materials integral to the findings presented in this article in accordance with the policy described in the Instructions for Authors (https://academic.oup.com/plcell/pages/General-Instructions) is Wenxiu Wang (wangwenxiu85@shnu.edu.cn).

Pedmale et al. 2016; Lian et al. 2018; Mao et al. 2021; Guo et al. 2023). The CCE domain mediates CRY1 signaling by interacting with COP1, an E3 ubiquitin ligase that regulates light signaling, and its enhancer SPAs (Deng et al. 1992; Hoecker et al. 1999; Seo et al. 2003). This interaction inhibits COP1-SPA activity, preventing the ubiquitination and degradation of substrates like HY5 via the 26S proteasome, thereby inhibiting skotomorphogenesis (Wang et al. 2001; Yang et al. 2001; Seo et al. 2004; Jang et al. 2010; Lian et al. 2011; Liu et al. 2011). HY5, a bZIP transcription factor, plays a central role in inhibiting skotomorphogenesis in darkness and promoting photomorphogenesis in response to light (Oyama et al. 1997). However, it remains unclear whether HY5 is degraded via the autophagy pathway or whether CRY1 regulates photomorphogenesis through autophagy inhibition.

Autophagy is a tightly regulated intracellular degradation pathway in eukaryotes, facilitated by a conserved set of AuTophaGy-related (ATG) proteins (Ohsumi 2014). In plants, over 30 ATG proteins form the core autophagy machinery, which is essential for stress adaptation, development, and defense (Marshall and Vierstra 2018; Qi et al. 2021). Among these, ATG8 (or Microtubule-Associated Protein 1 Light Chain 3 (LC3) in mammals) plays a central role in selective autophagy. When lipidated with phosphatidylethanolamine (PE), ATG8 regulates key stages of autophagy, including autophagosome formation, cargo recognition, and fusion with lysosomes or vacuoles (Nakatogawa et al. 2007; Nakatogawa 2013; Marshall and Vierstra 2018; Johansen and Lamark 2020). This lipidation is mediated by the E1- and E3-like enzyme activities of ATG5 and ATG7, making them critical components of the autophagy pathway (Hanada et al. 2007; Taherbhoy et al. 2011; Marshall and Vierstra 2018; Lamark and Johansen 2021). ATG8 directly interacts with specific substrates to mediate their autophagic degradation. For instance, Arabidopsis ATG8 targets S-nitrosoglutathione reductase 1 (GSNOR1) to regulate nitric oxide signaling (Zhan et al. 2018), while rice (Oryza sativa) ATG8 degrades Heading date 1 (Hd1) in the vacuole to control heading date (Hu et al. 2022). In mammals, LC3 interacts with nuclear proteins such as Sirt1 and Lamin B1, mediating their autophagic degradation to influence aging and tumorigenesis (Dou et al. 2015; Xu et al. 2020).

In this study, we show that CRY1 interacts with ATG8 in a blue light-dependent manner, inhibiting the interaction of ATG8 with HY5. The atg5 atg7 and atg8 mutants exhibit reduced skotomorphogenesis in darkness but enhanced photomorphogenesis under blue light, with being more pronounced with than without nutrient starvation. Moreover, ATG8 and ATG5/ATG7 act genetically downstream of CRY1, but upstream of HY5, to regulate photomorphogenesis. We further demonstrate that, in darkness, ATG8 and HY5 are co-localized to autophagosomes, leading to the autophagic degradation of HY5. Under blue light, CRY1 disrupts this process by inhibiting the ATG8-HY5 interaction. Moreover, we show that CRY1 mediates blue light inhibition of ATG8 export from the nucleus, as well as the formation of autophagosome. These findings suggest that the signaling mechanism of CRY1 involves inhibition of the selective autophagy of HY5, especially under nutrient starvation.

Results

CRY1 physically interacts with ATG8

Our screening for CRY1 N-terminus (CNT1)-interacting proteins using the GAL4 yeast two-hybrid system identified ATG8i, a key player in the selective autophagy pathway (Wang et al. 2018). We found that the full-length CRY1 interacted with ATG8i (Fig. 1A), and that CNT1 interacted with all 9 Arabidopsis ATG8s (ATG8a-i) to varying degrees in yeast cells, whereas the CCE domain of CRY1 did not (Supplementary Fig. S1). In vitro pull-down assays confirmed that both CNT1 and CRY1 interacted with ATG8a-i to varying degrees (Fig. 1B). Next, we focused on the wellstudied ATG8s, ATG8a, and ATG8e (Yoshimoto et al. 2004; Marshall et al. 2015; Qi et al. 2017; Liu et al. 2020), to determine the interaction of CRY1 with ATG8 in plants. We performed protein co-localization assays in Nicotiana benthamiana cells expressing ATG8a and ATG8e tagged with mCherry together with CNT1 tagged with YFP, respectively. The results showed that ATG8a and ATG8e co-localized with CNT1 in the same nuclear bodies (Fig. 1C), indicating their interactions in plant cells.

Next, we determined whether the interaction of CRY1 with ATG8 might be blue light-dependent. To this end, we first performed semi-in vivo pull-down assays and found that GST-ATG8a pulled down Myc-CRY1 from the transgenic Arabidopsis seedlings overexpressing Myc-CRY1 (Myc-CRY1-OX) exposed to blue light, but not from those either adapted in darkness or exposed to red or far-red light (Fig. 1D). Co-immunoprecipitation (co-IP) assays using N. benthamiana leaves transiently expressing Myc-CRY1 together with YFP-ATG8a or YFP-ATG8e, or YFP control, demonstrated the interaction of CRY1 with ATG8a or ATG8e in vivo (Fig. 1E). We then performed co-IP assays with transgenic Arabidopsis lines overexpressing ATG8a and ATG8e tagged with YFP in the wild-type (WT) background (YFP-8a-OX and YFP-8e-OX), respectively. As shown in Fig. 1, F and G, IP of YFP-ATG8a or YFP-ATG8e co-immunoprecipitated the endogenous CRY1 in the extract from YFP-8a-OX or YFP-8e-OX seedlings exposed to blue light, but did not in the extract from those adapted in darkness or from WT seedlings irradiated by blue light, indicating blue light-dependent interactions of CRY1 with ATG8a and ATG8e.

Typically, ATG8-binding proteins contain ATG8-interacting motifs (AIM) characterized by a W/F/Y-X-X-V/I/L consensus (Marshall and Vierstra 2018). We identified 4 putative AIM motifs in CRY1: YDPL (AA111-114), YPLV (AA341-344), WDTL (AA385-388), and WQYI (AA400-403). Yeast two-hybrid assay showed that Y111A L114A, Y341A V344A, and W400A I403A mutations within these AIM motifs compromised the interaction of CRY1 with ATG8i (Supplementary Fig. S2, A and B), respectively. Further split-LUC assays demonstrated that, although these mutations did not significantly affect CRY1 protein stability, they led to varying degrees of decrease in the interaction of CRY1 with ATG8a (Supplementary Fig. S2, C and D). As the AIM motif of ATG8-binding proteins often fits into the conserved LIR/AIM docking site (LDS) on ATG8 (Marshall and Vierstra 2018), we evaluated whether LDS would be required for the interaction of ATG8 with CRY1 by in vitro pulldown assay using mutant ATG8e comprising Y51A/L52A mutations within LDS (ATG8e^{mLDS}). The results showed that these mutations compromised the interaction of ATG8e with CRY1 (Supplementary Fig. S2E). We then generated the transgenic lines expressing the cassettes of cDNAs encoding WT CRY1 or CRY1 with AIM1 mutations (Y111A and L114A) under the control of CRY1 native promoter (Supplementary Fig. S3A) in cry1 mutant background (CRY1pro:CRY1/cry1 and CRY1pro:CRY1^{mAIM1}/cry1), respectively, with CRY1 and CRY1^{mAIM1} expressed at similar levels (Supplementary Fig. S3B). Hypocotyl growth analysis showed that AIM1 mutation compromised CRY1's capacity to rescue the cry1 mutant phenotype (Supplementary Fig. S3, C to F). Taken together, these results suggest that CRY1 may interact with ATG8 to regulate autophagy and hypocotyl elongation under nutrient starvation.

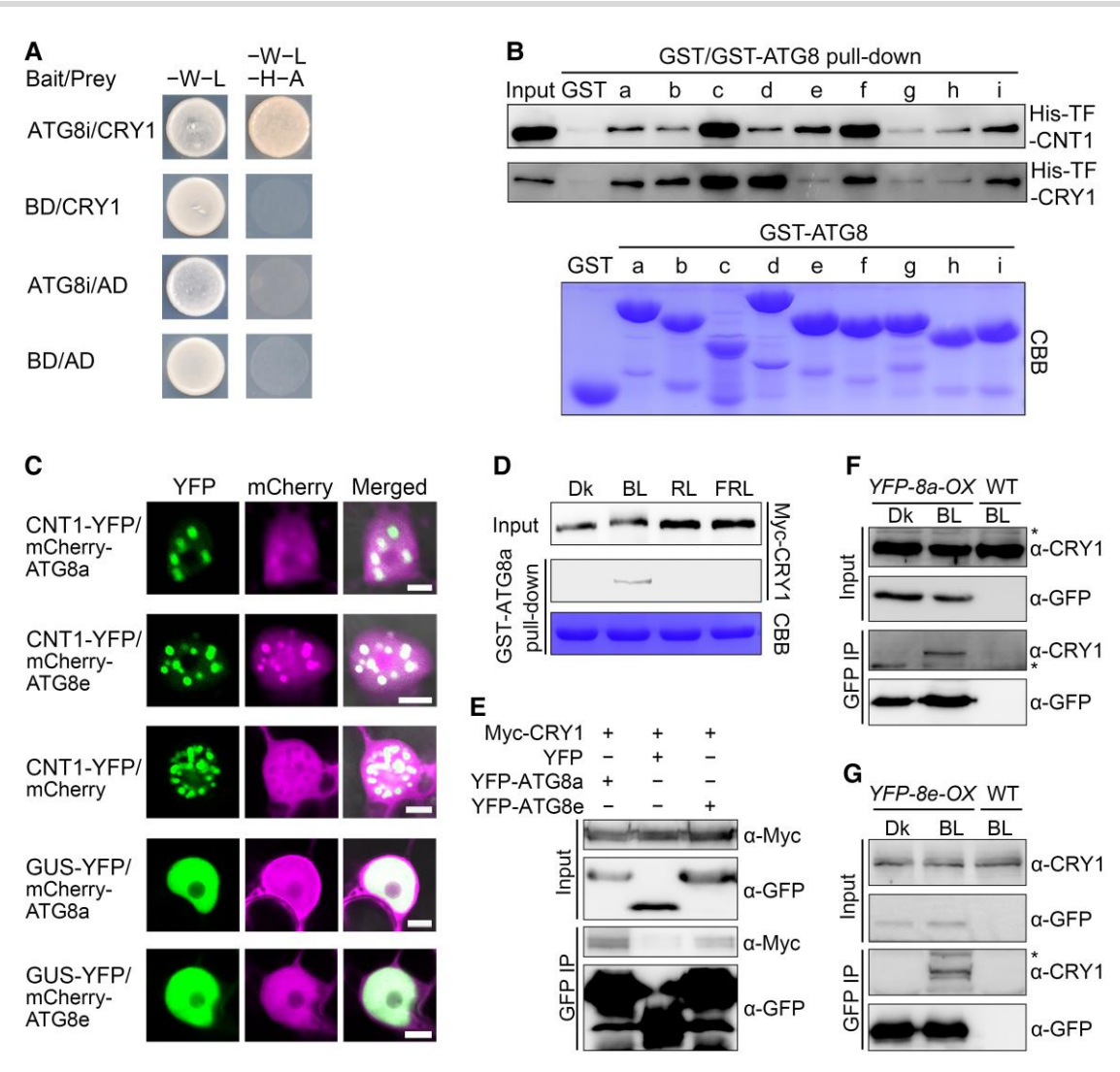


Figure 1. CRY1 interacts with ATG8 in a blue light-dependent manner. A) GAL4 yeast two-hybrid assay showing interaction of the full-length CRY1 with ATG8i. Yeast cells co-expressing the indicated combinations of constructs were grown on SD-Trp/Leu (-W-L) or SD-Trp/Leu/His/Ade (-W-L-H-A) under blue light (30 μ mol m⁻² s⁻¹). BD, GAL4 DNA-binding domain; AD, GAL4 DNA activation domain. B) In vitro pull-down assays showing the interactions of CNT1 and CRY1 with ATG8a-i. CBB, Coomassie Brilliant Blue staining. Letters a to i denote ATG8a to ATG8i. C) Protein co-localization assays indicating interactions of CNT1 with ATG8a/e in N. benthamiana cells. Bars, 5 μ m. D) Semi-in vivo pull-down assay showing blue light-specific interaction of CRY1 with ATG8a. Myc-CRY1-OX seedlings were adapted in darkness or exposed to blue (100 μ mol m⁻² s⁻¹) or red (20 μ mol m⁻² s⁻¹) or far-red (10 μ mol m⁻² s⁻¹) light for 1 h served as preys. CBB, Coomassie Brilliant Blue staining. Dk here and below in this figure, darkness; BL here and below in this figure, blue light; RL, red light; FRL, far-red light. E) Co-IP assay showing ATG8a/e-CRY1 interactions in N. benthamiana cells. Myc-CRY1 was co-expressed with YFP-ATG8a/e or YFP control. The IP (YFP-ATG8a/e and YFP) and co-IP signals (Myc-CRY1) were detected by immunoblots probed with anti-GFP and -CRY1 antibodies. IP, immunoprecipitation. Asterisks denote the nonspecific band recognized by anti-CRY1 antibody. At least 2 independent experiments were performed and the results were identical, and one of them is shown.

The autophagy pathway is involved in promoting skotomorphogenesis but inhibiting photomorphogenesis

As the ATG8-PE conjugation essential for autophagosome formation is dependent on ATG5 and ATG7 (Minina et al. 2018), atg5 or atg7 mutant may mimic atg8 mutant and is used in autophagy studies (Thompson et al. 2005; Lai et al. 2011). We therefore took atg5 and atg7 mutants to examine the possible skotomorphogenic and photomorphogenic phenotypes with or without nutrient (carbon and nitrogen) starvation (-C-N and +C+N), as plant autophagy is induced by carbon and/or nitrogen starvation (Doelling et al. 2002; Merkulova et al. 2014). The results showed that, in darkness, both atg5 and atg7 mutants developed significantly shorter

hypocotyls than WT with or without nutrient starvation, with being much more pronounced under nutrient starvation (Supplementary Fig. S4, A to D). Under blue light, atg5 and atg7 mutants exhibited a short hypocotyl phenotype under nutrient starvation only (Supplementary Fig. S4, E to H). Given that the hypocotyl elongation phenotype of the T-DNA insertion-mutagenized atg5 and atg7 mutants is not pronounced enough, we speculate that they may not be null mutants. Therefore, we constructed the atg5 atg7 double mutant. The results showed that the atg5 atg7 mutant exhibits a stronger short hypocotyl phenotype than atg5 or atg7 single mutants with or without nutrient starvation in darkness and blue light conditions, respectively (Fig. 2, A to H and Supplementary Fig. S4, E to H). These results indicate that ATG5 and ATG7 are involved in

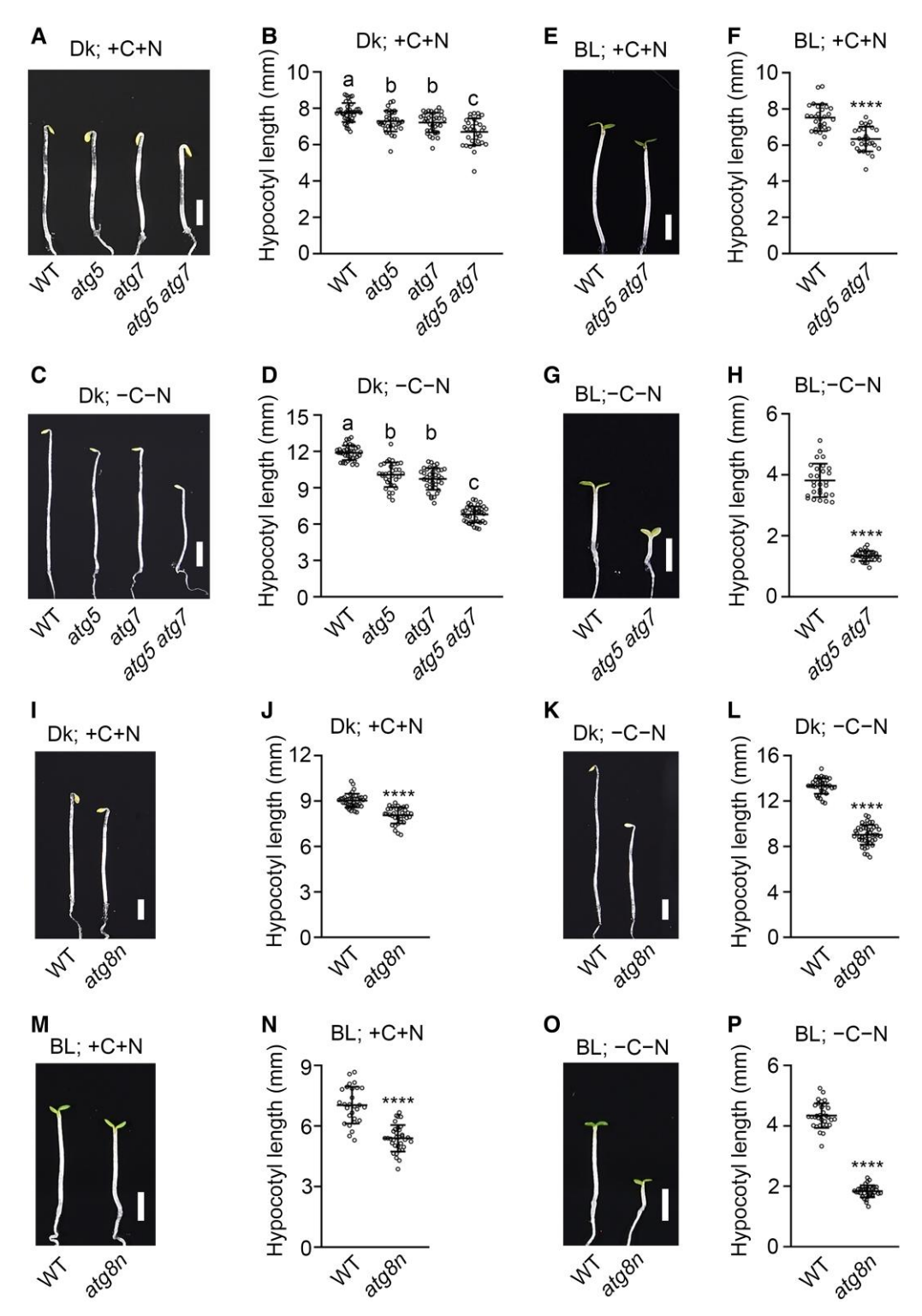


Figure 2. ATG5, ATG7, and ATG8 act to positively regulate hypocotyl elongation in low blue light. A to D) The atg5 atg7 mutant shows inhibited hypocotyl elongation with or without nutrient starvation in darkness. Scale bar here and below in this figure, 2 mm. +C + N denotes treatment without nutrient starvation here and below in this figure; C and N here and below in this figure, carbon and nitrogen; Dk here and below in this figure, darkness; BL here and below in this figure, blue light. E to H) The atg5 atg7 mutant shows inhibited hypocotyl elongation with or without nutrient starvation under blue light. I to L) The atg8n mutant shows inhibited hypocotyl elongation with or without nutrient starvation under blue light. I to L) The atg8n mutant shows inhibited hypocotyl elongation under blue light with or without nutrient starvation. Seedlings of the indicated genotypes were grown on MS+C+N or MS-C-N medium in darkness or blue light (1 μ mol m⁻² s⁻¹) for 4 d, and hypocotyl lengths were measured. Data in B, D, F, H, J, L, N, and P are shown as means \pm so $(n \ge 25)$. One-way ANOVA was applied to B and D, and different letters indicate significant differences among treatments (Tukey or Games-Howell test, P < 0.05). Student's t-test was used for F, H, J, L, N, and P (****P < 0.0001). At least 2 independent experiments were performed and the results were identical, and one of them is shown.

promoting skotomorphogenesis in darkness but inhibiting photomorphogenesis under blue light.

Next, we generated the knock-out nonuple mutant of ATG8a-i (atg8n) through CRISPR-Cas9 gene editing (Supplementary Fig. S5A). We found that, like the atq5 atq7 mutant, the atq8n mutant also showed a similar reduced skotomorphogenic phenotype in darkness but enhanced photomorphogenic phenotype under blue light with or without nutrient starvation, with being much more pronounced under nutrient starvation (Fig. 2, I to P), indicating ATG8's role in promoting skotomorphogenesis but inhibiting photomorphogenesis. We further determined the phenotype of a loss-of-function mutant of an upstream autophagy regulator, ATG11, with nutrient starvation treatment in darkness and blue light, respectively. The results showed that the atq11 mutant exhibited a similar promoted photomorphogenesis but inhibited skotomorphogenesis to atq5 atq7 and atq8n mutants (Supplementary Fig. S4, I to L). Taken together, these results suggest that the autophagy pathway is involved in promoting skotomorphogenesis in darkness but inhibiting photomorphogenesis under blue light.

ATG5/ATG7 and ATG8 act genetically downstream of CRY1 to regulate hypocotyl elongation

To determine the possible genetic interaction between ATG5/7/8 and CRY1 in regulating photomorphogenesis under blue light, we generated the cry1 atg5 atg7 triple mutant by genetic crossing and cry1 atg8n decuple mutant using CRISPR-Cas9 gene editing (Supplementary Fig. S5B). Phenotypic analysis revealed that the hypocotyls of both triple and decuple mutants were significantly shorter than cry1 single mutant, but taller than atq5 atq7 double and atg8n nonuple mutants under blue light with or without nutrient starvation, respectively, with being much more pronounced with nutrient starvation (Fig. 3), indicating that ATG5/ATG7 and ATG8 genetically act partially downstream of CRY1 to regulate photomorphogenesis. These results, in conjunction with the demonstration that CRY1 physically interacts with ATG8, suggest that CRY1 may mediate blue light regulation of photomorphogenesis, at least in part, through the ATG5/7/8-dependent autophagy pathway.

HY5 acts downstream of ATG5/7 and ATG8 to regulate hypocotyl elongation

Given that the autophagy pathway is involved in regulating hypocotyl growth and that HY5 is a pivotal transcriptional factor acting downstream from the multiple photoreceptors (Osterlund et al. 2000), we evaluated the genetic interactions of HY5 with ATG5/ ATG7 and ATG8 by constructing the atg5 atg7 hy5 triple mutant through genetic crossing and the atg8n hy5 decuple mutant using CRISPR-Cas9 gene editing (Supplementary Fig. S5C). The results showed that atg5 atg7 hy5 and atg8n hy5 hypocotyls were as tall as hy5 mutant in darkness with or without nutrient starvation and blue light without nutrient starvation (Fig. 4, A to F and I to N), respectively, and significantly taller than atg5 atg7 and atg8n mutant but shorter than hy5 mutant with nutrient starvation under blue light (Fig. 4, G, H, O, and P). These results suggest that HY5 genetically acts, at least partially, downstream of ATG5/ATG7 and ATG8 to regulate skotomorphogenesis in the dark and photomorphogenesis under blue light.

HY5 undergoes degradation via the autophagy pathway in darkness

To explore whether autophagy might regulate skotomorphogenesis by mediating HY5 autophagic degradation, we analyzed

endogenous HY5 protein levels with or without nutrient starvation. The results showed that HY5 was largely degraded in WT seedlings treated with nutrient starvation in darkness, but partially degraded in those treated without nutrient starvation in darkness (Supplementary Fig. S6A). We then examined HY5 levels in atg5 atg7 mutant and found that the accumulation of HY5 was substantially higher in atg5 atg7 mutant than in WT with nutrient starvation in darkness (Supplementary Fig. S6B). Moreover, the application of the autophagy inhibitors, E64d and ConA, clearly inhibited nutrient starvation-induced HY5 degradation in darkness (Supplementary Fig. S6C), demonstrating that the endogenous HY5 undergoes degradation through the autophagy pathway in darkness.

Next, we generated the transgenic line overexpressing HY5-GFP in WT background (HY5-GFP-OX) and analyzed HY5-GFP and free GFP levels in HY5-GFP-OX seedlings grown on nutrient-rich medium under white light for 3 d, and then treated with or without nutrient starvation in darkness for 24 h. We found that more HY5-GFP was degraded with than without nutrient starvation, with increased free GFP accumulation with than without nutrient starvation (Fig. 5A and Supplementary Fig. S6D). ConA application blocked nutrient starvation-induced HY5-GFP degradation and free GFP accumulation (Fig. 5B and Supplementary Fig. S6E). We further generated the transgenic line overexpressing HY5-GFP in atg5 atg7 mutant background (HY5-GFP-OX/atg5 atg7) and found that, upon 24 h nutrient starvation treatment in darkness, HY5-GFP was hardly degraded with or without ConA application (Supplementary Fig. S6F), and free GFP accumulation was also inhibited in the absence of ATG5 and ATG7 (Fig. 5C). Similarly, HY5-GFP degradation and free GFP accumulation were reduced in HY5-GFP-OX/atg8n under the same conditions (Fig. 5D). These results further confirm the autophagic degradation of HY5 in darkness. We also analyzed the accumulation of free YFP cleaved from YFP-ATG8e using YFP-8e-OX seedlings and found that YFP-ATG8e was degraded while free YFP accumulated upon 24 h nutrient starvation treatment in darkness (Fig. 5E), confirming that the nutrient starvation treatment used in this study is able to induce autophagy.

CRY1 mediates blue light inhibition of autophagic degradation of HY5

To determine if blue light inhibits the autophagy pathway, we analyzed the free YFP from YFP-ATG8e using YFP-8e-OX seedlings grown on nutrient-rich medium under white light for 3 d, and then treated with nutrient starvation in darkness or blue light for 24 h. The results showed that blue light illumination led to inhibition of YFP-ATG8e degradation and free YFP accumulation (Fig. 5F), indicating that blue light represses the autophagy pathway. We then investigated whether blue light might regulate the autophagic degradation of HY5 by analyzing endogenous HY5 and HY5-GFP levels in WT and HY5-GFP-OX seedlings under nutrient starvation in darkness or blue light, respectively. The results showed that much more HY5 or HY5-GFP was degraded with nutrient starvation in darkness than under blue light, while free GFP from HY5-GFP was lower in blue light than in the dark (Fig. 5G and Supplementary Fig. S6, G and I), indicating blue light inhibition of autophagic degradation of HY5. We then generated the transgenic line overexpressing HY5-GFP in cry1 background (HY5-GFP-OX/cry1) and explored whether CRY1 might mediate blue light inhibition of autophagic degradation of HY5 and HY5-GFP using cry1 mutant and HY5-GFP-OX/cry1 seedlings treated with nutrient starvation under blue light, respectively.

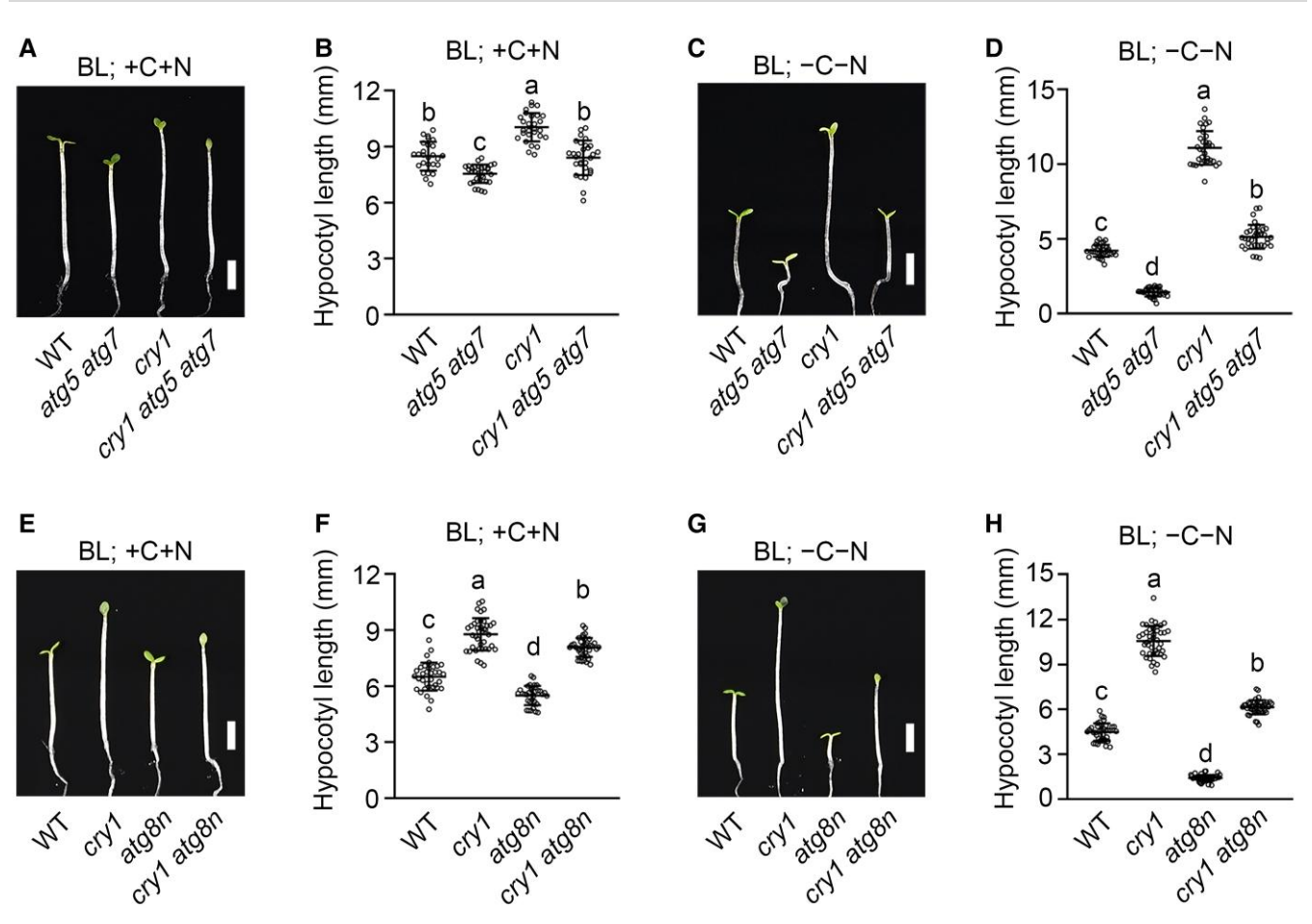


Figure 3. ATG5/7 and ATG8 act genetically downstream from CRY1 to regulate hypocotyl elongation. A to D) ATG5 and ATG7 act genetically downstream from CRY1 to regulate hypocotyl elongation with or without nutrient starvation under blue light. Scale bar here and below in this figure, 2 mm. +C + N denotes treatment without nutrient starvation here and below in this figure; BL here and below in this figure, blue light. E to H) ATG8 acts genetically downstream from CRY1 to regulate hypocotyl elongation with or without nutrient starvation under blue light. Seedlings of the indicated genotypes were grown on MS + C + N or MS - C - N medium in darkness or blue light (1 μ mol m⁻² s⁻¹) for 4 d, and hypocotyl lengths were measured. Data in B, D, F, and H are means \pm sD ($n \ge 25$). One-way ANOVA was applied, and different letters indicate statistically significant differences as determined by Tukey/Games-Howell's multiple testing methods (P < 0.05). At least 2 independent experiments were performed and the results were identical, and one of them is shown.

After 8 h nutrient starvation treatment under blue light, HY5 was largely degraded in cry1 mutant but hardly degraded in WT (Supplementary Fig. S6H), and that more HY5-GFP was degraded with more free GFP accumulating in HY5-GFP-OX/cry1 than in HY5-GFP-OX seedlings after 24 h nutrient starvation treatment under blue light (Fig. 5H and Supplementary Fig. S6J). Taken together, these results demonstrate that CRY1 is responsible for mediating blue light inhibition of autophagic degradation of HY5.

HY5 interacts directly with ATG8

Given the previous demonstration that ATG8 interacts with Hd1 in the nucleus and mediates its autophagic degradation (Hu et al. 2022) and our results showing that HY5 undergoes autophagic degradation and that HY5 acts genetically downstream from ATG8 to regulate hypocotyl growth, we asked whether ATG8 might interact with HY5. To test this, we first performed yeast two-hybrid assays using HY5 and its deletion fragments lacking the C-terminus containing bZIP region (HN1) or the N-terminus comprising COP1-interacting domain (HC1) (Osterlund et al. 2000; Lian et al. 2018) as baits, and ATG8a, ATG8e, and ATG8i as preys (Fig. 6A). The results showed that HY5 interacted with these

ATG8s, and that both HN1 and HC1 of HY5 were required for these interactions (Fig. 6B). Further in vitro pull-down assay revealed that ATG8a-i interacted with HY5 at different degrees, respectively (Fig. 6C and Supplementary Fig. S7A). It has been reported that ATG8 may interact with other proteins through the LDS or UDS (ubiquitin-interacting motif docking site) motifs (Marshall et al. 2015, 2019). In our study, we found that the I78A, F79A, and I80A mutations within the UDS domain of ATG8e significantly weakened the interaction between ATG8 and HY5, whereas Y51A/ L52A mutations within the LDS domain of ATG8e enhanced this interaction (Supplementary Fig. S7B). We further performed semiin vivo pull-down assays and found that GST-ATG8a or GST-ATG8e pulled down HY5-GFP from the protein extracts from HY5-GFP-OX seedlings, while GST did not (Fig. 6D). Co-IP assays using N. benthamiana leaves transiently expressing HY5-Flag together with YFP-ATG8a or YFP-ATG8e or YFP control demonstrated that HY5 interacted with ATG8a or ATG8e in vivo (Fig. 6E). Furthermore, we generated double transgenic lines overexpressing HY5-Flag together with YFP-ATG8a or YFP-ATG8e in WT background (HY5-Flag-OX/YFP-8a-OX or HY5-Flag-OX/ YFP-8e-OX), and performed co-IP assays using these and YFP-8a-OX or YFP-8e-OX seedlings grown under white light for

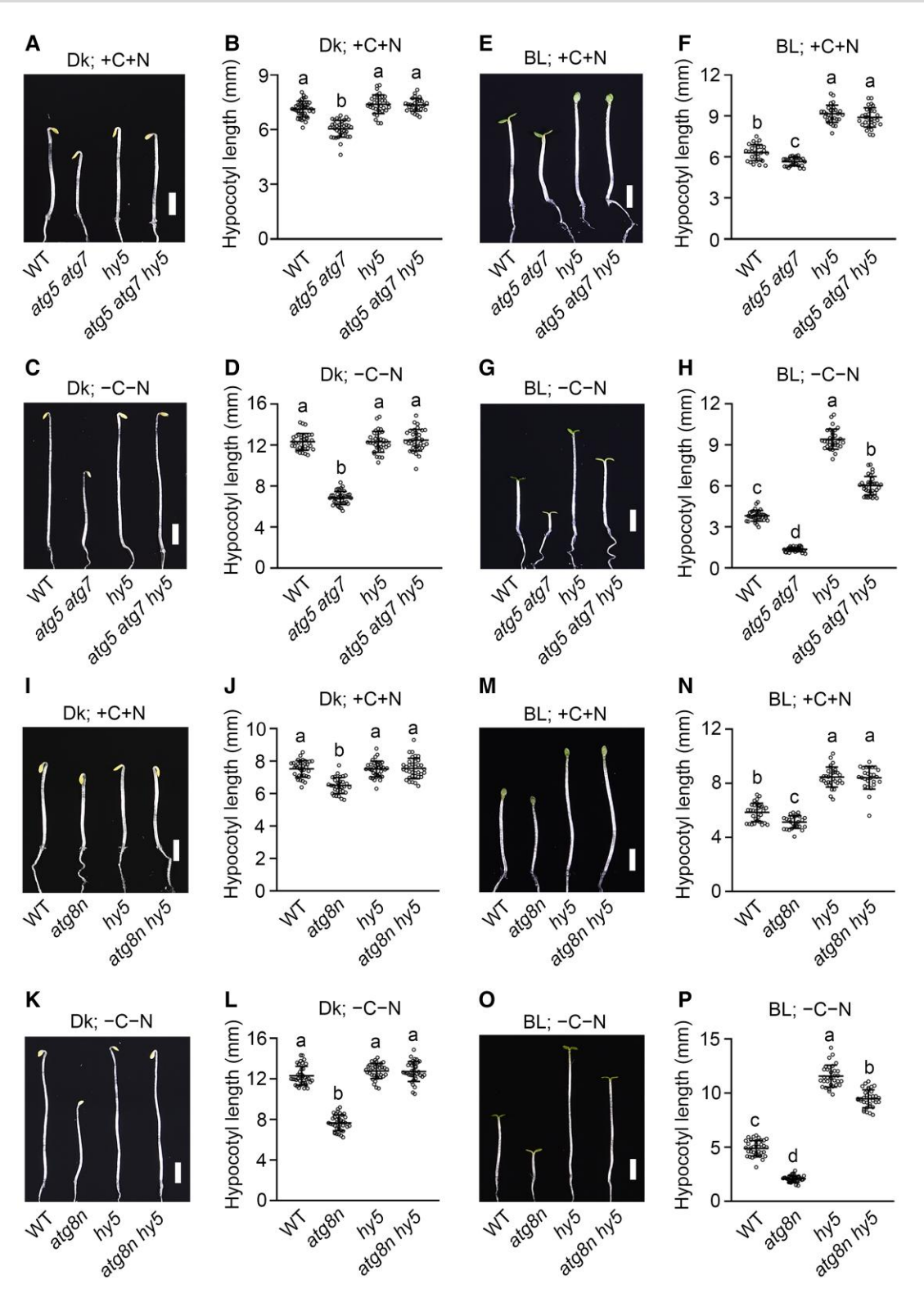


Figure 4. HY5 acts genetically downstream from ATG5/7 and ATG8 to regulate hypocotyl elongation. **A** to **D**) HY5 acts downstream from ATG5/7 to regulate hypocotyl elongation with or without nutrient starvation in darkness. Scale bar here and below in this figure, 2 mm. +C + N denotes treatment without nutrient starvation here and below in this figure; Dk here and below in this figure, darkness; BL here and below in this figure, blue light. **E** to **H**) HY5 acts downstream from ATG5/7 to regulate hypocotyl elongation with or without nutrient starvation under blue light. **I** to **L**) HY5 acts downstream from ATG8 to regulate hypocotyl elongation with or without nutrient starvation in darkness. **M** to **P**) HY5 acts downstream from ATG8 to regulate hypocotyl elongation with or without nutrient starvation under blue light. Seedlings of the indicated genotypes were grown on MS+C+N or MS-C-N medium in darkness or blue light $(1 \, \mu \text{mol m}^{-2} \, \text{s}^{-1})$ for 4 d, and hypocotyl lengths were measured. Data in **B**, **D**, **F**, **H**, **J**, **L**, **N**, and **P** are means $\pm \text{sd}$ ($n \geq 25$). One-way ANOVA was applied, and different letters indicate statistically significant differences as determined by Tukey/Games-Howell's multiple testing methods (P < 0.05). At least 2 independent experiments were performed and the results were identical, and one of them is shown.

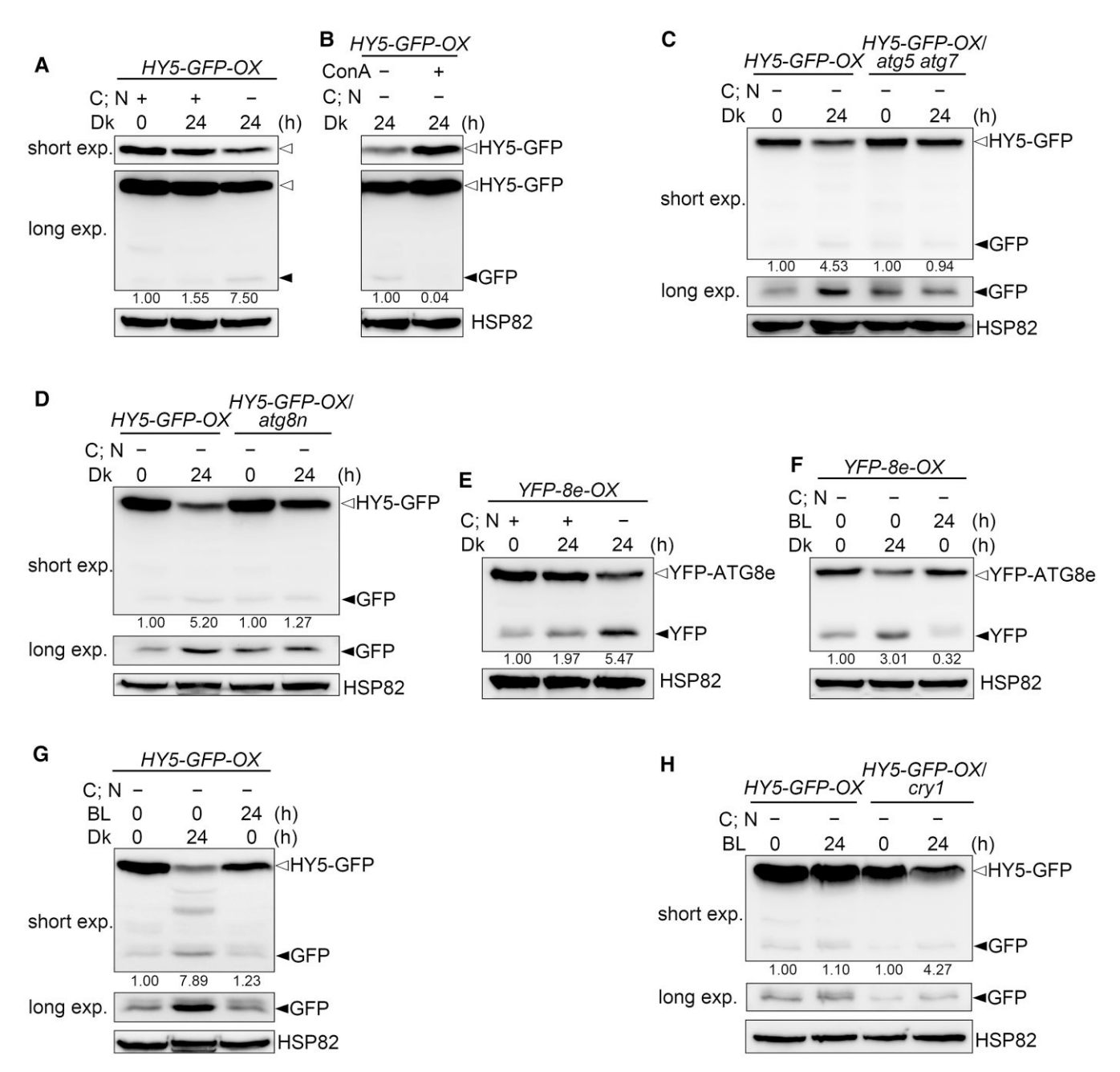


Figure 5. Free GFP assays confirm HY5 degradation through the autophagy pathway in darkness. A) Western blot assays showing more accumulation of free GFP released from HY5-GFP with than without nutrient starvation in darkness. C; N here and below in this figure, carbon and nitrogen; Dk here and below in this figure, Dark; Values below the blots here and below in this figure represent the ratio of free GFP to HY5-GFP fusion protein signals, and the first lane in each experiment was arbitrarily set to 1 to facilitate comparison. B) Western blot assays showing inhibition of accumulation of free GFP released from HY5-GFP by Cona. Cona, concanamycin A. C) Western blot assays showing inhibition of accumulation of free GFP released from HY5-GFP by ATG5 and ATG7 mutations. D) Western blot assays showing inhibition of accumulation of free GFP released from HY5-GFP by ATG8 mutation. E) Western blot assays showing more accumulation of free YFP released from YFP-ATG8e with than without nutrient starvation in darkness. Values below the blots here and below represent the ratio of free YFP to YFP-ATG8e fusion protein signals, and the first lane in each experiment was arbitrarily set to 1 to facilitate comparison. F) Western blot assays showing blue light inhibition of accumulation of free GFP released from HY5-GFP. H) Western blot assays showing CRY1 inhibition of accumulation of free GFP released from HY5-GFP. H) Western blot assays showing CRY1 inhibition of accumulation of free GFP released from HY5-GFP. H) Western blot assays showing CRY1 inhibition of accumulation of free GFP released from HY5-GFP and YFP-ATG8e fusion proteins were detected with anti-GFP antibody. HSP82 served as a loading control. The signals from the individual lanes were quantified by Imagel. Open arrowhead, GFP/YFP fusion; filled arrowhead, free GFP/YFP. At least 2 independent experiments were performed and the results were identical, and one of them is shown.

4 d, and then adapted in darkness for 2 h. As shown in Fig. 6, F and G, IP of HY5-Flag co-immunoprecipitated YFP-ATG8a and YFP-ATG8e in the extracts from HY5-Flag-OX/YFP-8a-OX and HY5-Flag-OX/YFP-8e-OX seedlings, but did not in those from YFP-8a-OX and YFP-8e-OX seedlings, demonstrating interaction of HY5 with ATG8 in Arabidopsis.

HY5 is co-localized with ATG8 to the autophagosome in darkness in an autophagy-dependent manner

Since HY5 interacts with ATG8 and undergoes autophagic degradation, we asked whether HY5 might be translocated from the nucleus to the autophagosome and vacuole for degradation. To verify

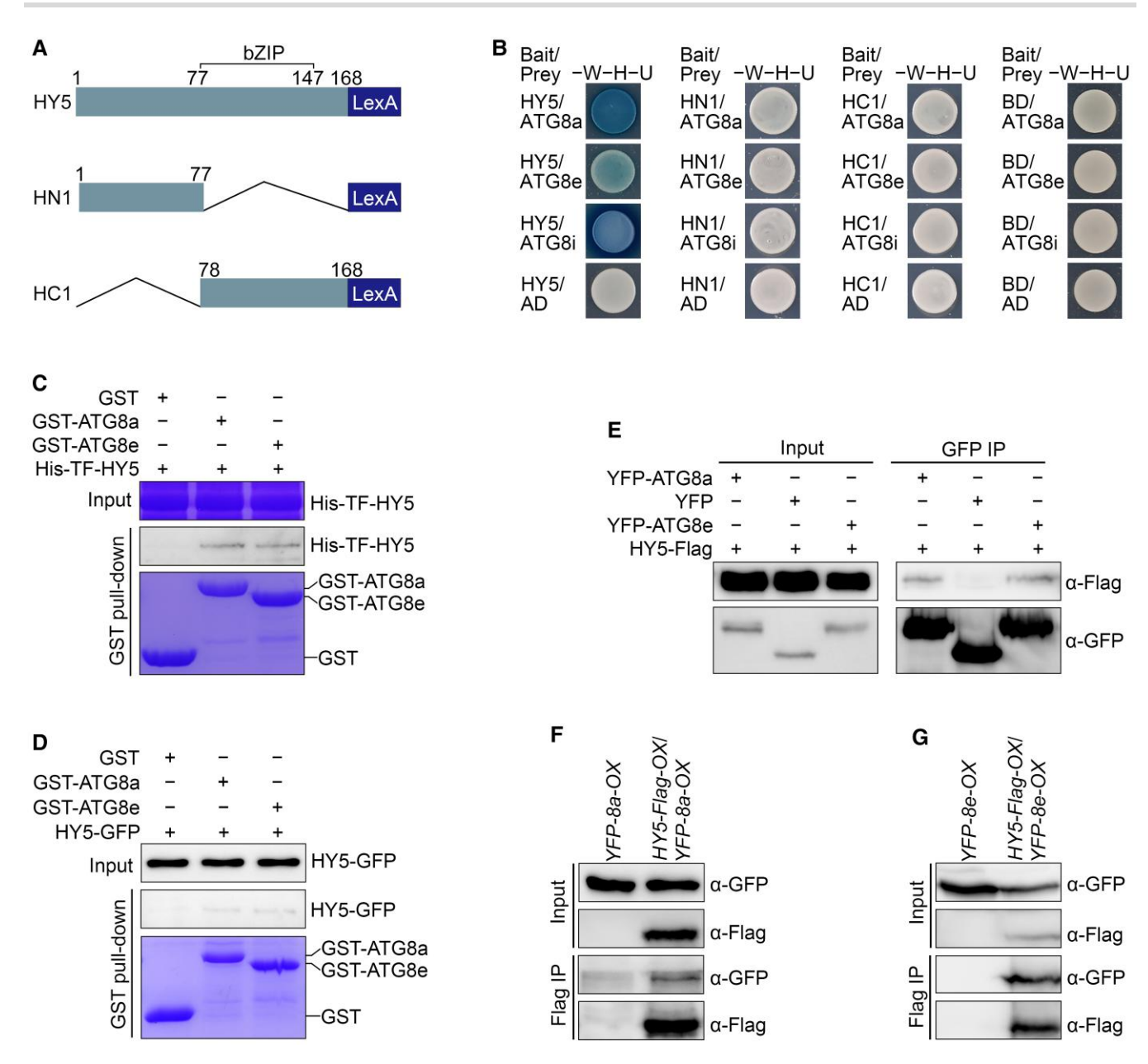


Figure 6. ATG8 interacts with HY5 in vitro and in vivo. A) Schematic diagrams displaying the yeast two-hybrid bait proteins. The bZIP domain of HY5 is indicated. B) LexA yeast two-hybrid assays showing the interactions of ATG8a/8e/8i with HY5 and the requirements of N- and C-termini of HY5 (HN1and HC1) for its interactions with these ATG8s. Yeast cells co-expressing the indicated combinations of constructs were grown on SD-Trp/His/Ura (-W-H-U) medium with X-gal. The blue precipitates on the plates represent the β-galactosidase activities. C) In vitro pull-down assays showing the interactions of HY5 with ATG8a and ATG8e. GST. ATG8a and GST-ATG8e served as baits, and His-TF-HY5 served as preys. Bait and the input of prey proteins denote Coomassie Brilliant Blue staining. D) Semi-in vivo pull-down assay showing the interaction of ATG8a and ATG8e with HY5. GST-ATG8a and GST-ATG8a served as baits, HY5-GFP extracts from dark-adapted HY5-GFP-OX seedlings served as preys. Bait protein denotes Coomassie Brilliant Blue staining. E) Co-IP assay showing ATG8a/e-HY5 interactions in N. benthamiana cells. HY5-Flag was co-expressed with YFP-ATG8a/e or YFP control. The IP (YFP-ATG8a/e and YFP) and co-IP signals (HY5-Flag) were detected by immunoblots probed with anti-YFP and HY5-Flag antibodies, respectively. F and G) Co-IP assays showing the interactions of ATG8a and ATG8e with HY5 in Arabidopsis. YFP-ATG8a/e-OX and HY5-Flag-OX/YFP-ATG8a/e-OX seedlings were grown in white light for 4 d, and then adapted in darkness for 2 h, and immunoprecipitated by anti-Flag antibody. The IP (HY5-Flag) and co-IP signals (ATG8a and ATG8e) were detected by immunoblots probed with anti-Flag and -GFP antibodies, respectively. At least 2 independent experiments were performed and the results were identical, and one of them is shown.

this possibility, we transiently expressed HY5-mCherry in WT Arabidopsis hypocotyl protoplasts treated with or without nutrient starvation in darkness in the presence of ConA, which increases vacuolar pH to stabilize the autophagosome in the vacuole that can be visualized by microscopy (Liu et al. 2020). Confocal microscopy showed that, without nutrient starvation, HY5-mCherry appeared to be exclusively localized in the nucleus. Strikingly, upon

nutrient starvation, a portion of HY5-mCherry was translocated to the numerous fluorescent puncta (Fig. 7A), resembling the autophagic bodies accumulating within the vacuole (Qi et al. 2017). To verify HY5 translocation from the nucleus, we then expressed HY5-mCherry with the nuclear-localized protein marker, H3-YFP, in hypocotyl protoplasts treated as above. The results showed that HY5-mCherry was co-localized with H3-YFP in the nucleus

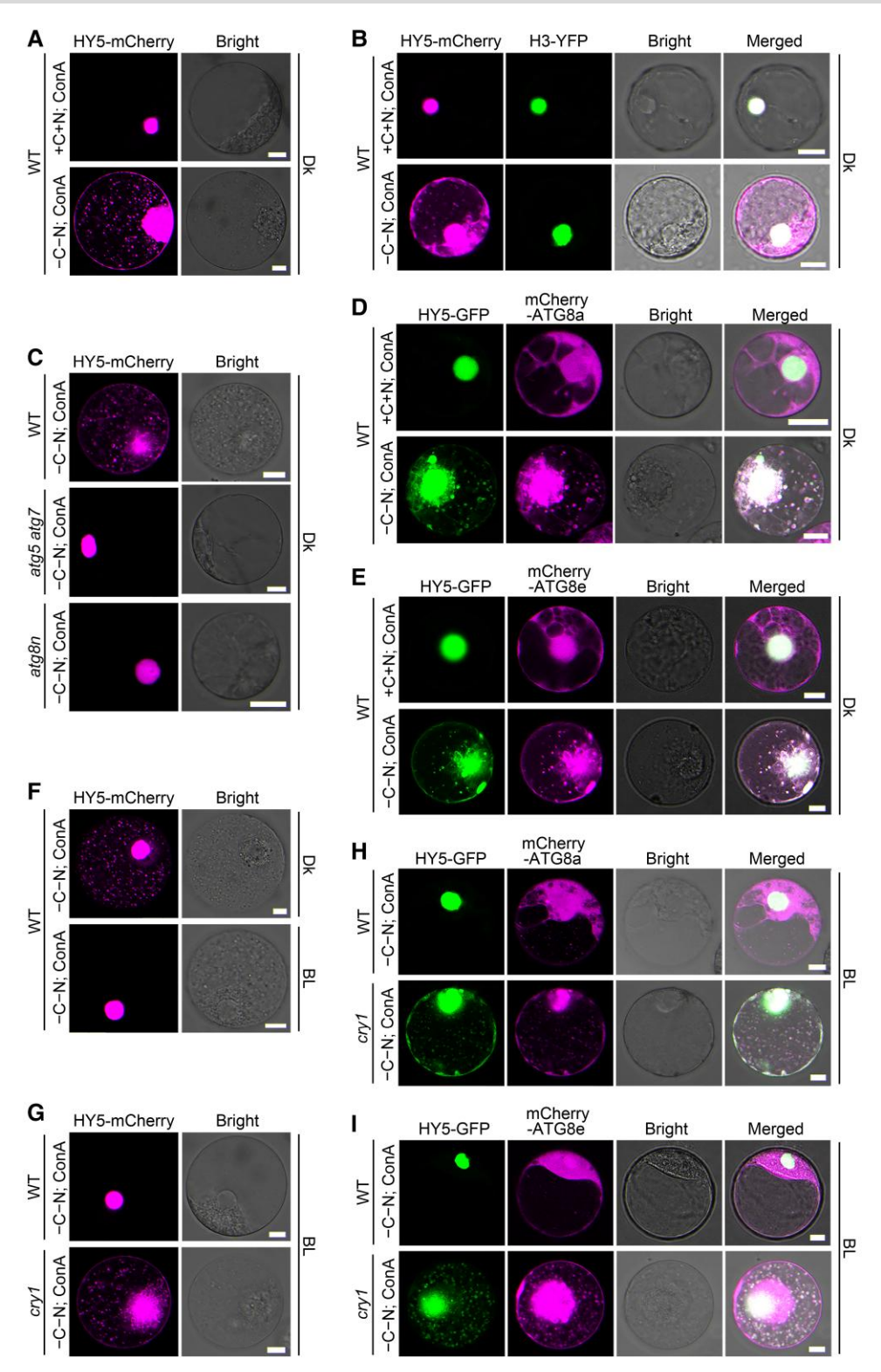


Figure 7. CRY1 mediates blue light inhibition of nutrient starvation-induced co-localization of HY5 with ATG8 to the autophagic bodies. A) Confocal microscopy images showing nutrient starvation-induced translocation of HY5-mCherry from the putative nucleus to the vacuole in darkness. Hypocotyl protoplasts were transfected with constructs expressing HY5-mCherry, and incubated in W5–C–N solution in darkness for 7 h before incubation in W5+C+N or W5–C–N solution with ConA and 24 h adaptation in darkness. Scale bar in this and other figures in this figure represents 10 μm. B) Confocal microscopy images showing that a portion of HY5-mCherry is translocated to the vacuole from the nucleus labeled by H3-YFP upon nutrient starvation in darkness. Protoplasts in WT background expressing HY5-mCherry and H3-YFP were incubated in W5+C+N or W5–C–N medium supplemented with ConA in darkness for 24 h. C) Confocal microscopy images showing that nutrient starvation induces translocation of HY5-mCherry from the nucleus to the vacuole in darkness in an autophagy-dependent manner. D and E) Confocal microscopy images showing nutrient starvation-induced co-localization of HY5-GFP with mCherry-ATG8a and mCherry-ATG8e to the autophagosome in darkness. F and G) Confocal microscopy images showing that blue light inhibits nutrient starvation-induced co-localization of HY5-mCherry from the nucleus to the vacuole is dependent on CRY1. H and I) Confocal microscopy images showing that blue light inhibits nutrient starvation-induced co-localization of HY5-GFP with mCherry-ATG8a and mCherry-ATG8e to the autophagosome in a CRY1-dependent manner. Confocal images were obtained from GFP and/or mCherry and/or bright field, and merged images are shown. Scale bar, 10 μm. At least 2 independent experiments were performed and the results were identical, and one of them is shown.

without nutrient starvation in darkness, whereas a portion of HY5-mCherry was translocated out of the nucleus upon nutrient starvation (Fig. 7B). To confirm whether the vacuolar puncta labeled by HY5-mCherry might indeed be of autophagic origin, we examined whether they would accumulate in atq5 atq7 and atq8n mutant protoplasts. As shown in Fig. 7C, these puncta were hardly seen in atg5 atg7 and atg8n mutant protoplasts, indicating that the puncta observed in the WT background are autophagosomes. These results therefore demonstrate that HY5 is likely localized to the autophagosome in darkness in an autophagy-dependent

To further confirm HY5's localization to the autophagosome under nutrient starvation, we expressed HY5-GFP together with the autophagosome marker, mCherry-ATG8a, or mCherry-ATG8e (Yoshimoto et al. 2004; Marshall et al. 2015; Marshall and Vierstra 2018; Liu et al. 2020), in WT hypocotyl protoplasts treated with or without nutrient starvation in darkness in the presence of ConA. The results showed that, without nutrient starvation, HY5-GFP was exclusively localized in the nucleus, while mCherry-ATG8a or mCherry-ATG8e was localized in both the nucleus and the autophagosome (Fig. 7, D and E). However, upon nutrient starvation, a portion of HY5-GFP was translocated to the autophagosome labeled by mCherry-ATG8a or mCherry-ATG8e and largely co-localized with mCherry-ATG8a or mCherry-ATG8e (Fig. 7, D and E). These findings confirm that HY5 is co-localized with ATG8 to the autophagosome in darkness in an autophagydependent manner.

CRY1 mediates blue light inhibition of autophagy-dependent co-localization of HY5 with ATG8 to the autophagosome

To investigate whether blue light might regulate HY5 vacuole localization, we analyzed its cellular localization using WT hypocotyl protoplasts expressing HY5-mCherry treated with nutrient starvation in darkness or blue light in the presence of ConA. As shown in Fig. 7F, the autophagic bodies were hardly seen within the vacuole under blue light, indicating blue light inhibition of HY5 translocation to the vacuole. To determine whether CRY1 might be involved in this process, we expressed HY5-mCherry in WT and cry1 mutant hypocotyl protoplasts treated with nutrient starvation under blue light in the presence of ConA, respectively. Confocal microscopy showed that numerous autophagic bodies were seen in cry1 mutant but not in WT (Fig. 7G), indicating a role for CRY1 in mediating blue light inhibition of HY5 translocation to the vacuole. We further confirmed CRY1's role using CRY1pro:CRY1/cry1 and CRY1pro:CRY1 $^{mAIM1}/cry1$ protoplasts, and found that the autophagic bodies were seen in CRY1pro: CRY1^{mAIM1}/cry1, but not in CRY1pro:CRY1/cry1 (Supplementary Fig. S8A), demonstrating that AIM1 is required for CRY1 inhibition of HY5's vacuole localization.

Next, we explored whether CRY1 might mediate blue light inhibition of the co-localization of HY5 with ATG8 using WT and cry1 mutant hypocotyl protoplasts expressing HY5-GFP, together with the mCherry-ATG8a or mCherry-ATG8e marker, which were treated with nutrient starvation under blue light in the presence of ConA. The results showed that, in the WT background, HY5-GFP was localized in the nucleus only, while mCherry-ATG8a or mCherry-ATG8e was localized in both the nucleus and autophagosome (Fig. 7, H and I), indicating blue light inhibition of the co-localization of HY5 with ATG8 to the autophagosome. In the cry1 mutant background, however, a portion of HY5-GFP was co-localized with mCherry-ATG8a or mCherry-ATG8e to the autophagosome (Fig. 7, H and I). We also

investigated whether cycloheximide (CHX) might affect blue light inhibition of the co-localization of HY5 with ATG8 in WT hypocotyl protoplasts. The results showed that CHX treatment did not alter the co-localization pattern of HY5-GFP and mCherry-ATG8e (Supplementary Fig. S8B), suggesting that their co-localization is independent of ongoing protein synthesis. These results demonstrate that CRY1 mediates blue light inhibition of the co-localization of HY5 with ATG8 to the autophagosome.

CRY1 mediates blue light inhibition of ATG8e export from the nucleus

Given that HY5 is translocated from the nucleus to the vacuolar puncta in an autophagy-dependent manner and that HY5 interacts and is co-localized with ATG8 in the autophagic bodies, we postulated that ATG8 might be localized in the nucleus, which is likely required for HY5 export from the nucleus. Indeed, we found that ATG8 was localized in the nucleus, as well as in the cytoplasm (Supplementary Fig. S9). We analyzed YFP-ATG8e levels in the nuclear and cytoplasmic fractions prepared from YFP-8e-OX seedlings with or without nutrient starvation in darkness or blue light. Results showed that more YFP-ATG8e accumulated in the nucleus without nutrient starvation under blue light than with nutrient starvation in darkness (Fig. 8A), indicating the negative effects of blue light and rich nutrients on ATG8e export from the nucleus. We then determined YFP-ATG8e levels in the nucleus using YFP-8e-OX seedlings treated with nutrient starvation in darkness or blue light, and found that more YFP-ATG8e accumulated in the nucleus under blue light than in darkness (Fig. 8B), indicating blue light inhibition of ATG8e export from the nucleus. To further investigate whether CRY1 might be involved in this process, we generated the transgenic line overexpressing YFP-ATG8e in cry1 mutant background (YFP-8e-OX/cry1) and examined YFP-ATG8e levels in the nucleus under nutrient starvation in darkness or blue light, with or without CHX. As shown in Fig. 8C and Supplementary Fig. S10A, more YFP-ATG8e accumulated in the nucleus of WT under blue light than in darkness, and more YFP-ATG8e accumulated in WT than in cry1 mutant nucleus under blue light, regardless of CHX treatment. Taken together, these results demonstrate that CRY1 mediates blue light inhibition of ATG8e export from the nucleus.

CRY1 mediates blue light inhibition of autophagosome formation

Given that ATG8 plays a critical role in autophagosome formation (Marshall and Vierstra 2018) and interacts with CRY1 (Fig. 1 and Supplementary Figs. S1and S2), we asked whether CRY1 would possibly be involved in regulating the formation of autophagosome. To test this, we analyzed autophagosome formation in YFP-8a-OX and YFP-8e-OX seedlings under nutrient starvation in darkness or blue light, with CHX and with or without ConA treatment, by confocal microscopy. The results showed that there were strikingly more autophagic bodies like puncta in root cells under darkness than blue light (Fig. 8, D to G). These puncta were autophagosomes, as they were barely seen in the transgenic line overexpressing YFP-ATG8e in atg5 atg7 mutant background (YFP-8e-OX/atq5 atq7) treated with nutrient starvation in darkness (Supplementary Fig. S10B). These results demonstrated that the formation of autophagosome was highly induced by dark but very strongly inhibited by blue light. To examine whether CRY1 might be involved in this process, we analyzed autophagosome formation in YFP-8a-OX/cry1 or YFP-8e-OX/cry1 seedlings treated with nutrient starvation under blue light in the presence of CHX

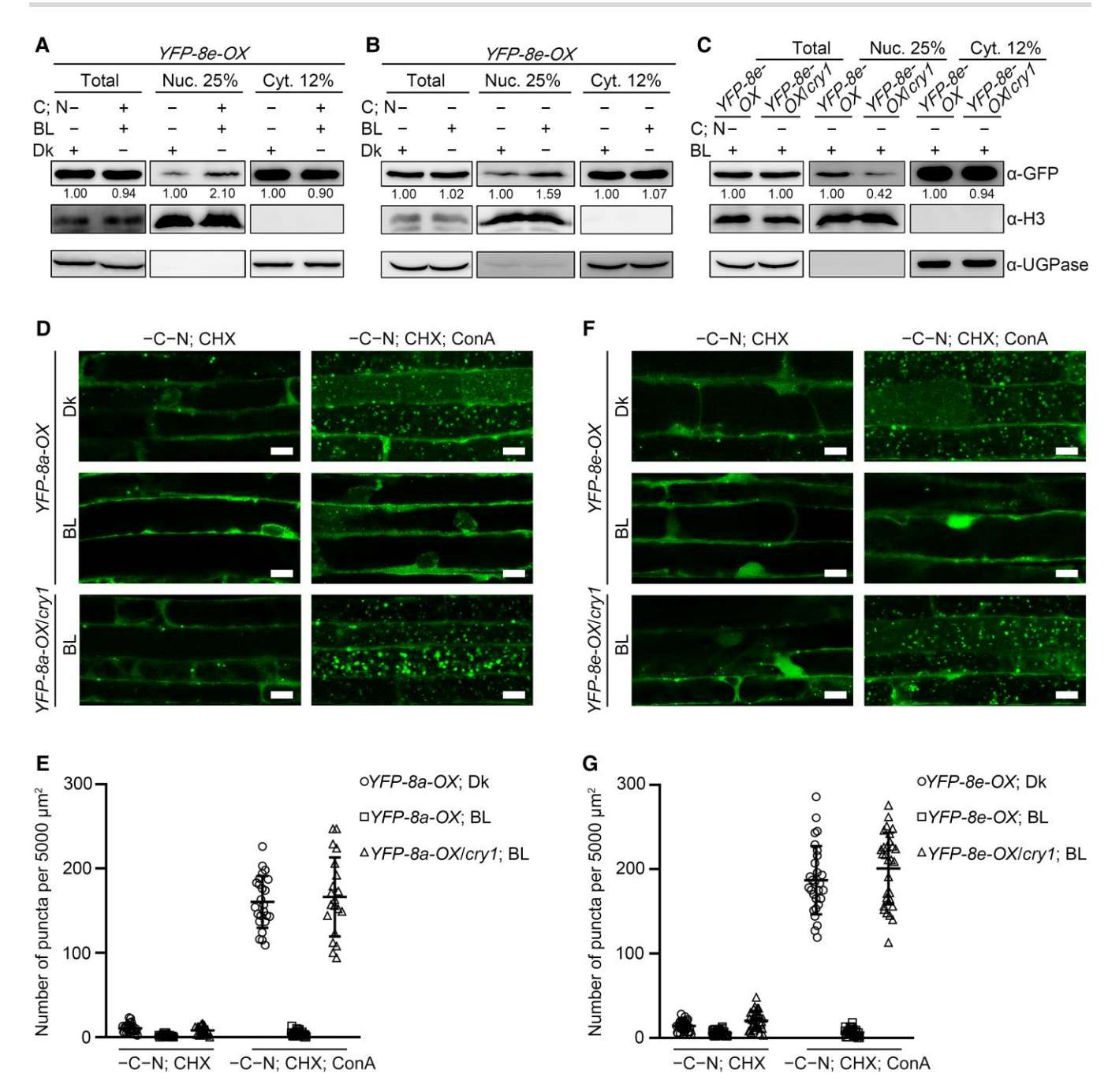


Figure 8. CRY1 inhibits ATG8 export from the nucleus and autophagic flux under nutrient starvation in blue light. A) Western blot analyses showing that more YFP-ATG8e is localized in the nucleus without nutrient starvation under blue light than with nutrient starvation in darkness. Nuc. 25% and Cyt. 12% here and below in this figure denote a total of 12% nuclear and 25% cytoplasmic proteins were loaded for Western blotting. C; N here and below in this figure, carbon and nitrogen; Dk here and below in this figure, Dark; BL here and below in this figure, blue light. Values below the blots in this figure represent protein levels normalized against the loading controls as quantified using ImageJ, and the first lane in each experiment was arbitrarily set to 1 to facilitate comparison. B) Western blot analyses showing that more YFP-ATG8e is localized in the nucleus with nutrient starvation under blue light than in darkness. C) Western blot analyses showing that more YFP-ATG8e is localized in the nucleus in the presence than in the absence of CRY1 with nutrient starvation under blue light. At least 2 independent experiments were performed and the results were identical, and one of them is shown. D and F) Confocal microscopy images showing that dramatically more autophagosomes labeled by YFP-ATG8e are produced in darkness than under blue light under nutrient starvation with CHX and ConA, and that significantly less autophagosomes are produced in the presence than in the absence of CRY1 under blue light. Scale bars, $10 \mu m$. —C—N denotes treatment with nutrient starvation here and below in this figure. E and G) Statistical analyses of the autophagic bodies shown in D and F. Data represent means (\pm sp) of more than 20 different optical areas from more than 10 individual seedlings' roots.

or ConA. The results showed that significantly more autophagosomes were produced in YFP-8a-OX/cry1 and YFP-8e-OX/cry1 than in YFP-8a-OX and YFP-8e-OX seedlings, respectively (Fig. 8, D to G). Taken together, these results demonstrate that CRY1 mediates blue light inhibition of the formation of autophagosome.

Photoexcited CRY1 inhibits the interaction of ATG8 with HY5

Given that CRY1 interacts with ATG8 in a blue light-dependent manner, and ATG8 interacts with HY5, we asked whether CRY1 would regulate ATG8-HY5 interaction under blue light. To test this possibility, we first performed semi-in vivo pull-down assays using His-TF-HY5 as bait, and protein extracts containing YFP-ATG8a and Myc-CRY1 from YFP-8a-OX/Myc-CRY1-OX seedlings exposed to blue light or adapted in the dark as prey and effector. The results showed that much less YFP-ATG8a was pulled down by His-TF-HY5 in blue light compared with darkness (Fig. 9A). Further semi-in vivo pull-down assays using GST-ATG8e as bait and His-TF-HY5 as prey showed that the capacity of GST-ATG8e binding to His-TF-HY5 was inhibited in the presence of Myc-CRY1 protein extracts from Myc-CRY1-OX seedlings illuminated by blue light (Fig. 9B). We also performed these assays using GST-ATG8e as bait and His-TF-HY5 as prev. and CRY1 and CRY1^{mAIM1} protein extracts from CRY1pro:CRY1/cry1 and CRY1pro:CRY1^{mAIM1}/cry1 seedlings exposed to blue light as effector, respectively. The results showed that AIM1 mutation compromised CRY1's capacity to inhibit ATG8e binding to HY5 (Fig. 9C). Co-IP assays using HY5-Flaq-OX/YFP-8a-OX or HY5-Flag-OX/YFP-8e-OX seedlings that were adapted in the dark or exposed to blue light. The results showed that blue light exposure led to reduced ATG8a-HY5 and ATG8e-HY5 interactions (Fig. 9, D and E). We then constructed the double transgenic line overexpressing both HY5-Flag and YFP-ATG8a in the cry1 mutant background (HY5-Flaq-OX/YFP-8a-OX/cry1), and performed a co-IP

assay using this genotype of seedlings adapted in the dark or exposed to blue light. We found that the ATG8a–HY5 interaction was less inhibited by blue light illumination in the absence of CRY1 than in the presence of CRY1 (Fig. 9E). Taken together, these results demonstrate that CRY1 mediates blue light inhibition of the interaction of ATG8 with HY5.

Discussion

HY5 undergoes degradation in darkness through the autophagy pathway

It has been demonstrated that HY5 undergoes degradation via the 26S proteasome pathway in darkness (Hardtke et al. 2000). In this study, we demonstrate that HY5 undergoes degradation through the selective autophagy pathway based on the following evidence: (i) Endogenous HY5 protein is degraded faster with than without nutrient starvation in darkness in an ATG5- and ATG7-dependent manner (Supplementary Fig. S6, A and B). Autophagy inhibitors repress its nutrient starvation-induced degradation (Supplementary Fig. S6C). (ii) HY5-GFP and YFP-ATG8e fusion proteins are also degraded faster with increased free GFP/YFP release with than without nutrient starvation in the dark (Fig. 5, A and E and

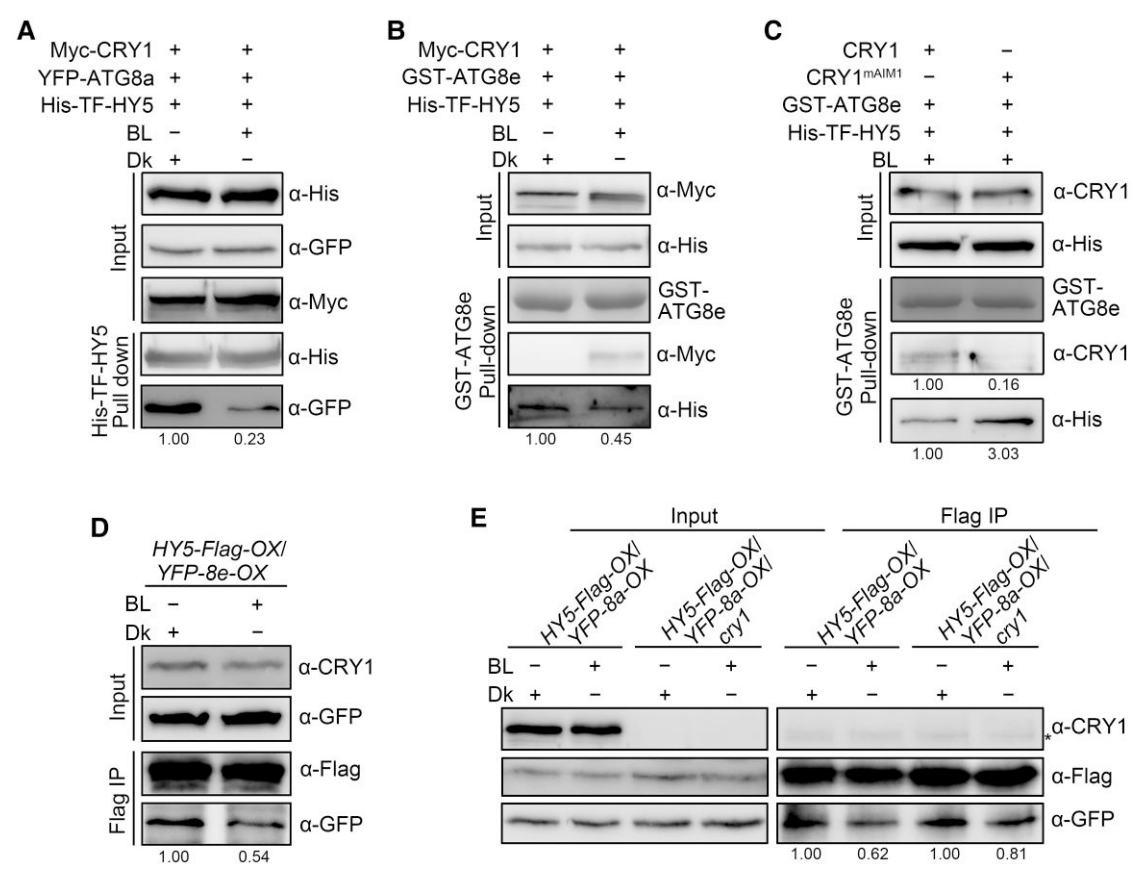


Figure 9. CRY1 inhibits the association of ATG8 with HY5 upon blue light irradiation. A and B) Semi-in vivo pull-down assays showing that CRY1 inhibits ATG8a–HY5 and ATG8e–HY5 interactions in a blue light-dependent manner. The bait, prey, and effector were detected with anti-His or -GFP or -Myc antibody. Dk here and below in this figure, Dark; BL here and below in this figure, blue light. Values below the blots in this figure represent protein levels normalized against the loading controls as quantified using ImageJ, and the first lane in each experiment was arbitrarily set to 1 to facilitate comparison. C) Semi-in vivo pull-down assay showing that AIM1 mutation compromises CRY1's capacity to mediate blue light inhibition of ATG8e–HY5 interaction. The bait, prey, and effector were detected with anti-His or -GFP or -CRY1 antibody. D) Co-IP assays showing blue light inhibition of the association of ATG8e with HY5 in Arabidopsis. E) Co-IP assay showing that CRY1 is involved in mediating blue light inhibition of the association of ATG8a with HY5 in Arabidopsis. The IP (HY5-Flag) and co-IP signals (ATG8a and ATG8e) were detected by Western blotting probed with anti-Flag and -GFP antibodies, respectively. Asterisks denote the nonspecific band recognized by anti-CRY1 antibody. At least 2 independent experiments were performed and the results were identical, and one of them is shown.

Supplementary Fig. S6D). Either application of the autophagy inhibitor or loss-of-function of ATG5, ATG7, and ATG8 leads to inhibition of nutrient starvation-induced HY5-GFP degradation and free GFP accumulation (Fig. 5, B to D and Supplementary Fig. S6, E and F). (iii) ATG5, ATG7, and ATG8 play a more important role in regulating skotomorphogenesis and photomorphogenesis with than without nutrient starvation, partially dependent on HY5 (Figs. 2 and 4). (iv) HY5 directly interacts with ATG8 (Fig. 6). (v) Upon nutrient starvation, HY5 translocates from the nucleus and is co-localized with ATG8 to the autophagosome in darkness (Fig. 7, A to E).

Given that MG132 treatment inhibited HY5 degradation under nutrient starvation in darkness, and that the atq mutants failed to completely suppress the degradation of endogenous HY5 and HY5-GFP fusion protein (Fig. 5, C and D; Supplementary Figs. S6, B and C and S12C), we postulate that the 26S proteasome pathway may play a role in mediating HY5 degradation during autophagy induction. COP1 is a master negative regulator of photomorphogenesis, which mediates HY5 ubiquitination and degradation via the 26S proteasome pathway (Hardtke et al. 2000; Osterlund et al. 2000), and HY5 degradation is largely inhibited in cop1 mutant seedlings, indicating that the degradation of HY5 is likely primarily dependent on COP1-mediated ubiquitination. As the autophagic degradation of substrate proteins of the autophagy pathway such as the pivotal brassinosteroid signaling component BES1, and the plant growth and drought resistance regulator constitutively stressed 1 (COST1) is dependent on their ubiquitination modification (Nolan et al. 2017; Bao et al. 2020; Wang et al. 2021a), it will be interesting to investigate whether COP1-meidated HY5 ubiquitination is required for its autophagic degradation in future studies.

The signaling mechanism of CRY1 involves inhibition of the autophagic degradation of HY5

Arabidopsis CRY1 regulates many aspects of plant growth and development by interacting with key factors from multiple signaling pathways, such as Aux/IAA, ARF, BES1, and DELLA proteins in phytohormone signaling (Wang and Lin 2020, 2025; Qu et al. 2024). Our findings reveal a mechanism by which blue light signaling, mediated by CRY1, regulates the autophagy pathway to regulate photomorphogenesis. In this study, we reveal that the signaling mechanism of CRY1 involves the inhibition of the selective autophagy of HY5 based on the following lines of evidence. (i) CRY1 interacts with ATG8 in a blue light-dependent manner (Fig. 1, D, F, and G), leading to inhibition of the ATG8-HY5 interaction (Fig. 9, A to E). (ii) The atg5 atg7 and atg8n mutants show a more pronounced enhanced photomorphogenic phenotype under blue light with than without nutrient starvation (Fig. 2, E to H and \mbox{M} to P), and ATG5, ATG7, and ATG8 act genetically downstream of CRY1 to regulate photomorphogenesis (Fig. 3). (iii) AIM1 mutation compromises CRY1's capacity to interact with ATG8 and inhibit its interaction with HY5, and rescue the cry1 tall-hypocotyl phenotype and inhibit HY5 vacuole localization (Fig. 9C and Supplementary Figs. S2, S3, and S8A). (4) CRY1 mediates blue light inhibition of autophagic degradation of HY5 and free GFP accumulation (Fig. 5, G and H and Supplementary Fig. S6, G to J). (5) CRY1 mediates blue light inhibition of HY5 translocation from the nucleus to the vacuole and disruption of the co-localization of HY5 with ATG8 to the autophagosome (Fig. 7, F to I). Based on these demonstrations, we speculate that the autophagy pathway is involved in CRY1-mediated blue light signaling with or without nutrient starvation, with being more involved under nutrient deficiency.

It is known that the CNT domain of CRYs can bind to flavin adenine dinucleotide (FAD) and absorb light, but CCE cannot. Crystal structure studies show that, upon sensing blue light through their N-termini, CRYs undergo dimerization/oligomerization, leading to the formation of interaction surfaces in their N-termini (Shao et al. 2020), which may enable CCE also to form interaction surfaces. These interaction surfaces may enable CRYs to interact with a variety of their interacting proteins, such as COP1, SPAs, Auxs/ IAAs, ARFs, BES1, DELLAs, TOE1/TOE2, PIFs, and ADA2b (Wang et al. 2001, 2018; Yang et al. 2001; Lian et al. 2011; Liu et al. 2011; Xu et al. 2018; Du et al. 2020; Mao et al. 2020; Xu et al. 2021; Zhong et al. 2021). In this study, we reveal that ATG8s are CNT1-interacting proteins, and that AIM1, AIM2, and AIM4 motifs within CNT1/CRY1-PHR may be involved in mediating the interaction with ATG8 (Supplementary Fig. S2, A to D). We further modeled the potential tetramer structure of AtCRY1-PHR based on the ZmCRY1c cryo-EM structure (Shao et al. 2020) and found that the 4 AIM motifs are located near the surface of CRY1 (Supplementary Fig. S11). Specifically, AIM1 lies within the α/β domain, and AIM2 is situated near the conserved CRY1 INT1 region, possibly mediating the interaction with downstream signaling partners (Shao et al. 2020). However, both AIM3 and AIM4 are positioned at the W400-containing FAD-binding pocket related to light responsiveness (Gao et al. 2015). AIM3 appears not to be involved in CRY1-mediated regulation of the autophagy pathway. Given that CRYs and the other photoreceptors interact with the same downstream components, including COP1, to mediate light signaling (Wang et al. 2001; Yang et al. 2001; Seo et al. 2004; Favory et al. 2009; Jang et al. 2010), it will be interesting to explore whether the other photoreceptors may also interact with ATG8 to regulate HY5 degradation through the autophagy pathway.

We demonstrate that CRY1 mediates blue light inhibition of nutrient starvation-induced ATG8 translocation from the nucleus (Fig. 8, A to C). Given ATG5- and ATG7-dependent HY5 translocation from the nucleus to the vacuole and nutrient starvationdependent co-localization of HY5 with ATG8 to the autophagosome in darkness (Fig. 7, C to E), we speculate that ATG8-HY5 interaction may be required for HY5 export from the nucleus to the vacuole. Blue light-induced interaction of CRY1 with ATG8 in the nucleus may, on the one hand, inhibit the translocation of ATG8 from the nucleus to the cytoplasm (Fig. 8, A to C and Supplementary Fig. S10A), and may, on the other hand, inhibit HY5 translocation from the nucleus by interfering with the interaction of HY5 with ATG8 in the nucleus (Fig. 9, A to E). How exactly CRY1 may inhibit ATG8 export from the nucleus awaits further investigation. We noticed that the change in nuclear ATG8e levels appeared not to affect cytosolic ATG8e levels, possibly because the absolute levels of ATG8e in the cytosol are high, and a mild change in nuclear ATG8e hardly influences cytosolic ATG8e levels. A similar phenomenon is observed for OGDH2 and phyB that undergo cytoplasmic-nuclear translocation (Huang et al. 2023; Zhao et al. 2023).

It is intriguing to reveal in this study that remarkably more autophagosomes were produced in the dark than under blue light, and that CRY1 is responsible for mediating blue light inhibition of the formation of autophagosome (Fig. 8, D to G). As CRY1 is present in both the nucleus and cytoplasm (Yang et al. 2000; Wu and Spalding 2007), we speculate that the cytoplasm-localized CRY1 may interact with ATG8 under blue light to inhibit the formation of autophagosome by interfering with its function in promoting phagophore expansion and/or closure. Given the essential roles of ATG4, ATG5, and ATG7 in promoting formation of the ATG8-PE conjugate (Yoshimoto et al. 2004; Thompson et al. 2005; Romanov et al. 2012; Bu et al. 2020),

it will be worth exploring whether the interaction of CRY1 with ATG8 may interfere with the interactions of ATG8 with these ATG proteins to disrupt PE attachment to ATG8 and inhibit the formation of autophagosome.

Autophagy and 26S proteasome pathways may coordinate HY5 degradation

Why is HY5 degraded through both the 26S proteasome and the autophagy pathways? After seeds germinate under the soil, these 2 pathways may work simultaneously to ensure highly efficient degradation of HY5. As a result, the young seedlings are able to elongate rapidly and penetrate the soil before the limited nutritional substances stored in the seeds run out, and then capture the sunlight, undergo photomorphogenesis, and carry out photosynthesis. To determine possible dynamic autophagic degradation of HY5 during skotomorphogenesis, we monitored HY5-GFP accumulation in WT and atq5 atq7 mutant backgrounds at different time points after seed germination in the dark or blue light with or without nutrient starvation, respectively. We found that, in the WT background, HY5-GFP levels were not very different at 48 h post-germination (hpg) in the dark and blue light with or without nutrient starvation, and at 72 hpg, they were similar in darkness and blue light without nutrient starvation, while much lower in the dark than under blue light with nutrient starvation. Without nutrient starvation, clear HY5-GFP degradation was seen till 120 hpg. With nutrient starvation, however, HY5-GFP was largely degraded at 96 hpg, and almost totally degraded at 120 hpg. By contrast, in the atg5 atg7 mutant background, HY5-GFP was very stable in the dark with nutrient starvation, as even till 120 hpg, it was clearly detectable (Supplementary Fig. S12). These results suggest that both autophagy and 26S proteasome pathways are involved in mediating HY5 degradation during skotomorphogeneis, with the former being more involved under nutrient starvation.

In nature, as there may exist varied degrees of nutrient deficiency in the soil, germinated seedlings may face different levels of nutrient starvation, which may trigger different levels of autophagy. The higher the degree of nutrient deficiency, the higher the level of autophagic degradation of HY5. Given that atg5 atg7 and atg8n mutants show reduced skotomorphogenic phenotype in darkness but enhanced photomorphogenic phenotype under blue light with or without nutrient starvation (Fig. 2), the autophagy pathway must be always involved in dark and blue light control of skotomorphogenesis and photomorphogenesis, with being more involved under nutrient starvation but less involved under less or no nutrient starvation. This means that, even under less or no nutrient starvation and blue light, a small portion of ATG8 and HY5 may be translocated to the autophagosome and degraded in the vacuole.

It has been reported that HY5 recruits Histone Deacetylase 9 (HDA9) to ATG5 and ATG8e loci, linking light signaling to autophagy at the transcriptional level during the light-to-dark transition (Yang et al. 2020). Our study demonstrates that, under nutrient starvation in darkness, HY5 is degraded through the autophagy pathway, which may relieve its repression of ATG gene expression by inhibiting HDA9 recruitment. In contrast, under blue light, the autophagic degradation of HY5 is inhibited, which may lead to enhanced interaction with HDA9 and suppression of ATG genes' transcription. Such bidirectional regulation suggests that light and nutrient signals may coordinately fine-tune autophagy to precisely regulate photomorphogenesis under changing environmental conditions. Furthermore, previous studies have shown that HY5 acts as a mobile transcription factor coordinating carbon and nitrogen acquisition between shoots and roots (Chen et al.

2016). In this study, we found that HY5 undergoes nuclear export and autophagic degradation under nutrient starvation in darkness, which is suppressed by blue light-activated CRY1 (Figs. 5 and 7), thereby likely allowing HY5 to mediate the light-dependent coordination of shoot growth and carbon assimilation with root development and nitrogen acquisition. This regulatory mechanism may provide a cellular basis for the shoot-to-root signaling role of HY5, and together, these findings highlight the multifaceted roles of HY5 in nutrient sensing and systemic coordination.

A model

Based on the results obtained in the present study, we propose a working model concerning how CRY1 promotes photomorphogenesis through the regulation of selective autophagy of HY5. In darkness, CRY1 is monomerized and inactive, thus unable to interact with ATG8 in both the cytosol and nucleus. Cytoplasmic ATG8 may be fully capable of promoting autophagosome formation, while the nuclear-localized ATG8 and HY5 interact and are translocated to the autophagosome and vacuole for degradation (Fig. 10A). Upon blue light irradiation, CRY1 undergoes dimerization/oligomerization, gets activated, and is able to interact with ATG8 in both the cytosol and the nucleus. As a result, on the one hand, ATG8 activity in promoting autophagosome formation in the cytosol may be inhibited, and on the other hand, the interaction of ATG8 with HY5 in the nucleus is inhibited, and the translocation of HY5 from the nucleus to the vacuole is inhibited (Fig. 10B). The regulation of HY5 protein stability by the dynamic interactions of CRY1 with ATG8 and ATG8 with HY5 defined in the present study provides a dynamic signaling mechanism by which plants fine-tune the level of selective autophagy of HY5 to optimize skotomorphogenesis and photomorphogenesis according to the light and nutrient conditions.

Based on the findings obtained in this study, it is interesting to hypothesize that, in darkness, ATG8 may also interact with its other substrates and mediate their autophagic degradation, while under blue light, CRY1 may inhibit their autophagic degradation by inhibiting their interactions and the formation of autophagosome. If so, blue light may regulate a variety of autophagy-controlled physiologic processes, such as plant growth and development, and plant adaptation to biotic and abiotic stresses, through CRY1. Given that low blue light induces starvation responses to promote autophagy and hypocotyl growth under shade (Ince et al. 2022), it will be interesting to explore whether CRY1 is possibly involved in mediating shade response through the regulation of autophagy. CRY and ATG8 are conserved in plants and mammals, and it is shown that the interaction of LC3 with CRY1 leads to autophagic degradation of CRY1 in mice (Toledo et al. 2018). Given that the CRYs-COP1 interactions in Arabidopsis can inhibit COP1 activity, and conversely mediate CRYs degradation via the 26S proteasome (Wang et al. 2001; Yang et al. 2001; Lian et al. 2011; Liu et al. 2011, 2022; Ma et al. 2021; Miao et al. 2022), it will be interesting to investigate whether the CRYs-ATG8 interactions may conversely mediate CRYs degradation via selective autophagy pathway in Arabidopsis and whether LC3-CRY1 interaction may conversely affect LC3 activity and the degradation of its other substrates through selective autophagy pathway in mammals.

Materials and methods Plant material and growth conditions

The Arabidopsis thaliana (Col-0 ecotype) cry1, hy5, atg5, atg7, and atg11 mutants, and the transgenic lines overexpressing Myc-CRY1

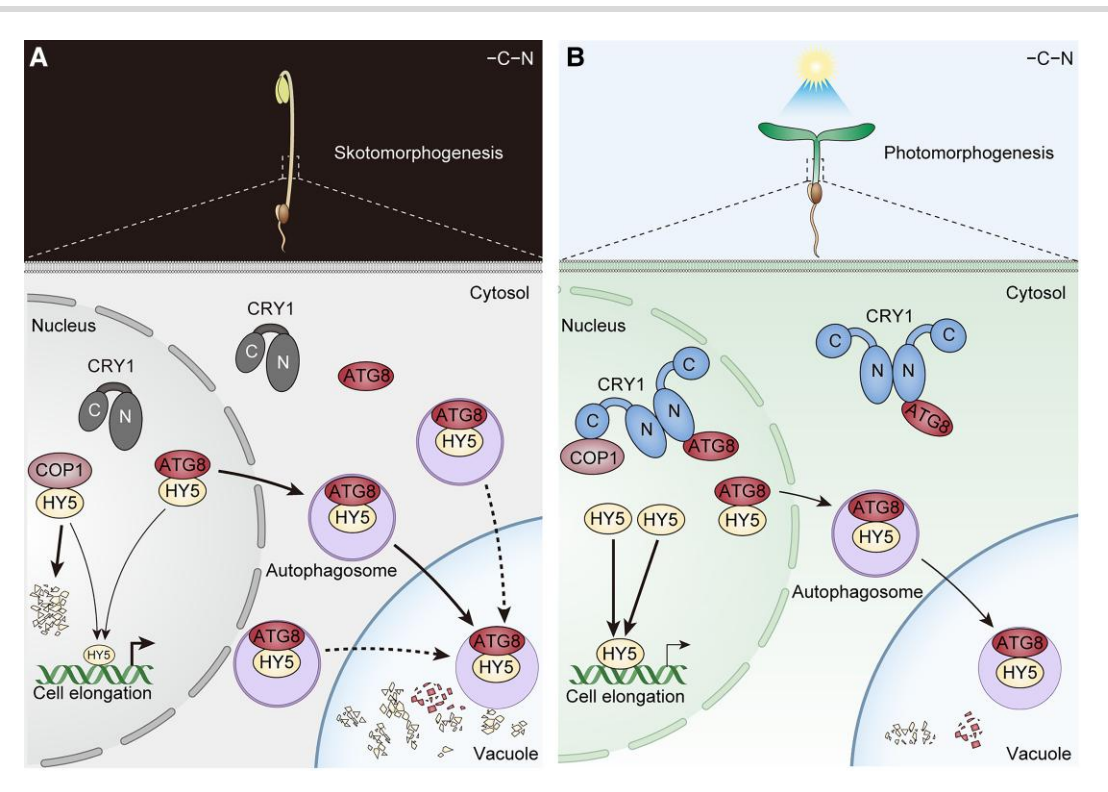


Figure 10. A model illustrating how CRY1 inhibits the autophagic degradation of HY5 in response to blue light. A) In darkness, CRY1 is in monomer and inactive, and unable to interact with ATG8. The nuclear-localized ATG8 and HY5 interact and are largely translocated to the autophagosome and vacuole for degradation (thick arrows). Meanwhile, the cytoplasm-localized ATG8 is capable of promoting the formation of autophagosome. As a result, little HY5 accumulates in the nucleus, and the genes promoting cell elongation inhibited by HY5 are highly expressed (thick arrow), leading to skotomorphogenesis. B) Under blue light, CRY1 undergoes dimerization/oligomerization and is able to interact with ATG8 in both the nucleus and cytosol. Consequently, ATG8 and HY5 hardly interact in the nucleus and are barely translocated to the autophagosome and vacuole for degradation (thin arrows). At the same time, ATG8 activity in the cytosol is inhibited by CRY1, leading to inhibition of autophagosome formation. Therefore, HY5 highly accumulates (thick arrows) and the genes promoting cell elongation are hardly expressed (thin arrow), resulting in photomorphogenesis. -C-N denotes treatment with nutrient starvation.

(Myc-CRY1-OX) were described previously (Yang et al. 2000; Alonso et al. 2003; Mao et al. 2005; Sang et al. 2005; Jia et al. 2014; Huang et al. 2019; Young et al. 2019). The ATG8a-i nonuple mutant (atg8n), cry1 atg8n, and atg8n hy5 decuple mutants were generated in this study using the CRISPR-Cas9 gene editing system (Wang and Chen 2020) and confirmed by DNA sequencing. The atg5 atg7 double, and cry1 atg5 atg7 and atg5 atg7 hy5 triple mutants were generated by genetic crossing. The expression cassettes 35S: HY5-GFP and 35S:YFP-ATG8a-i were cloned into pCambia1300-GFP and pCambia1300-YFP vectors, respectively. Then, they were transformed into the WT background to generate transgenic lines overexpressing HY5-GFP and YFP-ATG8a-i (HY5-GFP-OX and YFP-8a-i-OX). The transgenic lines overexpressing Myc-CRY1 and YFP-ATG8a in WT background (YFP-8a-OX/Myc-CRY1-OX), and HY5-GFP, YFP-ATG8a, and YFP-ATG8e in atg5 atg7 or cry1 mutant background (HY5-GFP-OX/cry1, HY5-GFP-OX/atg5 atg7, YFP-8a-OX/ cry1, YFP-8e-OX/cry1, YFP-8e-OX/atq5 atq7) were generated by genetic crossing. The expression cassettes CRY1pro:CRY1 and CRY1pro: $CRY1^{mAIM1}$ were cloned into pCambia1300 vector, respectively, and then transformed into cry1 mutant background to generate the CRY1pro:CRY1/cry1 and CRY1pro:CRY1^{mAIM1}/cry1 lines. The expression cassette 35S:HY5-Flag was cloned in pHB vector (Mao et al. 2005) and then transformed into YFP-8a-OX, YFP-8e-OX, and YFP-8a-OX/cry1 lines to generate the double transgenic lines coexpressing HY5-Flag and YFP-ATG8a or YFP-ATG8e in WT and cry1 mutant backgrounds (HY5-Flag-OX/YFP-8a-OX, HY5-Flag-OX/ YFP-8e-OX, and HY5-Flag-OX/YFP-8a-OX/cry1), respectively. The primers for vector construction are listed in Supplementary Data Set 1. Different genotypes of seedlings were grown on MS micronutrient (MSP18-10LT, Jianglai Biological) supplemented with 3 mm CaCl₂, 1.5 mm MgSO₄, 1.25 mm KH₂PO₄, 5 mm KCl, 2 mm MES, 20.6 mm NH₄NO₃, and 18.8 mm KNO₃ and 2% sucrose (pH 5.7) (MS+C+N) or MS micronutrient supplemented with 3 mm CaCl₂, 1.5 mm MgSO₄, 1.25 mm KH₂PO₄, 5 mm KCl, (pH 5.7) (MS-C-N) (Thompson et al. 2005; Chung et al. 2009), or in soil at 22 °C under white light (100 μ mol m⁻² s⁻¹). All plates were kept at 4 °C in darkness for 3 d for stratification and then transferred to a 22 °C incubator under white light for 8 h for further analysis. Experiments involving blue light illumination were described previously (Wang et al. 2018). Light spectra and intensity were measured with a HandHeld spectroradiometer (ASD) and a Li250 quantum photometer (Li-Cor).

Hypocotyl length measurements

Hypocotyl lengths were measured using ImageJ. Student's t-test (2 independent sample t-test) for 2 independent groups was performed using SPSS, with significant differences indicated as ****P < 0.001. Other statistical differences were calculated by one-way ANOVA. Different letters indicate statistically significant differences as determined by Tukey/Games-Howell's multiple testing methods (P < 0.05). Mean \pm sp. $n \ge 25$. All the statistical analyses are provided in Supplementary Data Set 2.

Yeast two-hybrid assay

The GAL4 yeast two-hybrid screening, construction of the BD-CNT1, BD-CCE1, and AD-CRY1 vectors, and yeast two-hybrid

assays were described previously (Wang et al. 2018). The cDNA fragment of ATG8i was cloned into pGBKT7 vector, and the fragments encoding ATG8a-i and the mutated CRY1s comprising mutations in the putative AIM motifs were cloned into pGADT7 vector, respectively. Combinations of BD and AD vectors were cotransformed into AH109 cells via the PEG/LiAc transformation procedure. Transformed yeast cells were spread on SD plates lacking Trp, Leu, His, and Ade (SD-W-L-H-A) supplemented with 5 or 25 mm 3-AT for the interaction test.

For LexA yeast two-hybrid assays using EGY48 yeast cells (Lian et al. 2011), the cDNA sequence encoding HY5 was cloned into pLexA-JL (Li et al. 2021), to generate the vectors expressing HY5-LexA, HN1-LexA, and HC1-LexA, which were co-transformed with pB42AD vectors expressing B42AD-ATG8a, B42AD-ATG8e, and B42AD-ATG8i, respectively. Transformed colonies were selected on SD-W-H-U medium. Six independent clones were taken and grown on SD-W-H-U medium with 0.2 mm X-gal (TaKaRa) for the interaction assay. The primers for vector construction are listed in Supplementary Data Set 1.

In vitro pull-down assays

Construction of His-TF-CNT1 and His-TF-CRY1 cassettes was described previously (Xu et al. 2021). The cDNAs encoding ATG8a-i, ATG8e^{mLDS}, and ATG8e^{mUDS} were cloned into pGEX-4T-1 vector, respectively. All the proteins were expressed in E. coli (Rossita). The bait proteins GST-ATG8a-i, GST-ATG8e^{mLDS}, GST-ATG8e^{mUDS}, or GST were incubated with GST beads (GE) in lysis buffer (50 mm Tris-HCl, pH 7.5, 150 mm NaCl, 0.2% Triton-X-100) at 4 °C for 2 h, and washed 3 times with the same buffer. The beads were then resuspended in 1 mL lysis buffer, and 50 to 100 ng of prey proteins His-TF-CNT1, His-TF-CRY1, His-TF-HY5, and His-TF were added, respectively. The mixture was incubated at 4 °C for 1 h and then washed 3 times. Bait proteins were visualized by Coomassie brilliant blue staining, and prey proteins were detected by Western blotting using anti-His antibody (Genscript). The primers for vector construction are listed in Supplementary Data Set 1.

Semi-in vivo pull-down assays

For blue light-specific CRY1-ATG8a interaction assays, GST-ATG8a bait proteins were first incubated with 10 μ L GST agarose beads for 1 h and then washed 3 times with lysis buffer, respectively. The protein extracts from Myc-CRY1-OX seedlings used as preys, which were grown on white light for 4 d, and then adapted in darkness for 2 d followed by 1 h dark adaptation of or exposure to blue light (100 μ mol m⁻² s⁻¹) or red light (20 μ mol m⁻² s⁻¹) or far-red light $(10 \, \mu \text{mol m}^{-2} \, \text{s}^{-1})$. Prey proteins were detected using anti-Myc antibody (Abclonal).

For assays of HY5-ATG8a/ATG8e interaction, HY5-GFP-OX seedlings were grown in white light for 3 to 4 d, and then adapted to darkness for 2 h. GST-ATG8a, GST-ATG8e, or GST bait proteins were first incubated with GST beads for 1 h, and then washed 3 times with lysis buffer, respectively. The protein extracts from HY5-GFP-OX seedlings were used as prey. Bait proteins were visualized by Coomassie brilliant blue staining, and prey proteins were detected by Western blotting using anti-GFP (Abmart) antibodies.

For assays of CRY1 effects on ATG8a-HY5 interaction, His-TF-HY5 bait protein was incubated with 10 μ L His agarose beads for 1 h, and then washed 3 times with lysis buffer. The protein extracts containing YFP-ATG8a and Myc-CRY1 prepared from YFP-8a-OX/Myc-CRY1-OX seedlings were used as preys and effectors, which were grown in white light for 4 d, and then adapted in darkness for 2 d, followed by 1 h dark adaptation or blue light exposure (100 μ mol m⁻² s⁻¹). Prey and bait proteins were detected using anti-GFP and -His antibodies, respectively.

For assays of CRY1 effects on ATG8e-HY5 interaction, GST-ATG8e bait protein was incubated with 10 μ L GST agarose beads for 1 h, and then washed 3 times. The beads were resuspended in 1 mL non-EDTA buffer, and 50 to 100 ng His-TF-HY5 prey protein was added. The protein extracts prepared from Myc-CRY1-OX or CRY1pro:CRY1/cry1 or CRY1pro:CRY1^{mAIM1}/cry1 seedlings served as effectors, which were grown in white light for 4 d, and then adapted in darkness for 2 d, followed by 1 h dark adaptation or blue light exposure (100 μ mol m⁻² s⁻¹). Bait proteins were visualized by Coomassie brilliant blue staining, and prey proteins were detected using anti-His antibodies.

All the seedlings were homogenized with lysis buffer supplemented with 1 mm pefabloc (Roche) and cocktail (Roche), and $50 \, \mu \text{M}$ MG132 (MCE). After centrifugation, the supernatant was incubated with the beads used in the assays for 30 min and washed 3 times with lysis buffer, and then, the precipitates were eluted into 20 µL SDS 1x loading buffer and subjected to Western

Protein co-localization study

The construction of 35:CNT1-NLS-YFP and 35S:GUS-NLS-YFP cassettes was described previously (Wang et al. 2018). The cassettes comprising 35S:mCherry-ATG8a/e cassettes were cloned into pCambia1300-mCherry vector, respectively. GV3101 cultures harboring the constructs expressing mCherry- and YFP-fusion proteins, and p19 were mixed at a ratio of 1:1:1 and infiltrated into N. benthamiana leaves. Protein co-localizations were detected by confocal microscopy (Leica Stellaris 8). YFP and mCherry were excited using 514 nm (5% intensity, gain: 4 to 120 V) and 587 nm (10% to 40% intensity, gain: 30 to 130 V) lasers, respectively, with emission signals collected at 519 to 541 nm (YFP) and 596 to 625 nm (mCherry). The primers for vector construction are listed in Supplementary Data Set 1.

Split-luciferase (LUC) assays

Construction of the vectors expressing cLUC-CRY1 and CRY1-nLUC was described previously (Du et al. 2020). The cDNAs encoding ATG8a and the mutated CRY1s comprising mutations in the putative AIM motifs were amplified and cloned into the pCambia1300-nLUC and pCambia1300-cLUC (Du et al. 2020), respectively. GV3101 culture mixtures harboring the constructs expressing the nLUC- and cLUC-fused proteins were introduced into N. benthamiana leaves and the luciferase signal were analyzed as described previously (Xu et al. 2021). The primers for vector construction are listed in Supplementary Data Set 1.

Co-immunoprecipitation (co-IP) assays

For co-IP assays of CRY1-ATG8a and CRY1-ATG8e interactions, YFP-8a-OX and YFP-8e-OX or WT seedlings were grown in white light for 4 to 5 d, followed by 2 d adaptation in darkness. Then, WT and one-half of YFP-8a-OX and YFP-8e-OX seedlings were exposed to blue light (100 μ mol m⁻² s⁻¹) for 1 h, whereas the other half remained in darkness for 1 h. For co-IP assays of ATG8a-HY5 and ATG8e-HY5 interactions, HY5-Flag-OX/YFP-8a-OX and YFP-8a-OX or HY5-Flag-OX/ YFP-8e-OX and YFP-8e-OX seedlings were grown in white light for 3 to 4 d and then adapted in darkness for 2 h. For co-IP assays of CRY1 inhibition of the interactions of HY5 with ATG8a and ATG8e, HY5-Flag-OX/YFP-8a-OX, HY5-Flag-OX/YFP-8e-OX, and HY5-Flag-OX/ YFP-8a-OX/cry1 seedlings were grown in white light for 3 to 4 d, and then adapted in darkness for 2 h. One-half of these genotypes of

seedlings were exposed to blue light (100 μ mol m⁻² s⁻¹) for 1 h, while the other half remained in darkness for 1 h. The seedlings treated above were harvested in dim green safe light and homogenized in the lysis buffer. Total protein concentration was determined by Bradford assay (Bio-Rad), and equal amounts of total protein in lysis buffer were incubated with anti-GFP or anti-Flag agarose beads (Sigma) at 4 °C for 2 h. The IP were washed 3 times with the wash buffer and subjected to Western blot analyses with antibodies against the CCE domain of CRY1 (Sang et al. 2005) or Flag or GFP.

The construction of the vector expressing Myc-CRY1 and YFP for co-IP assays in N. benthamiana leaf cells was described previously (Wang et al. 2018; Xu et al. 2018). YFP, YFP-ATG8a, and YFP-ATG8e proteins were co-expressed with Myc-CRY1 or HY5-Flag in N. benthamiana leaves for anti-GFP IP, respectively. Equal amounts of total protein in lysis buffer from N. benthamiana leaf cells were incubated with anti-GFP or anti-Flag agarose at 4 °C for 2 h. The IPs were washed 3 times with the wash buffer and subjected to Western blot analyses with anti-Myc and anti-GFP antibodies.

Autophagic protein degradation assays

WT, atg5 atg7, cry1, HY5-GFP-OX, HY5-GFP-OX/atg5 atg7, HY5-GFP-OX/cry1, and YFP-8e-OX seedlings were grown on MS+C +N medium in white light (100 μ mol m⁻² s⁻¹) or far-red light $(1 \mu \text{mol m}^{-2} \text{ s}^{-1})$ for 3 d, and then transferred into liquid MS + C + N and/or MS-C-N medium supplemented with or without autophagy inhibitors 3-MA (5 mm) (Selleck), E64d (50 μm) (Apexbio), ConA (5 µm) (Abcam), and 26S proteasome inhibitor MG132 (50 µM), and then adapted in darkness or exposed to blue light $(90 \,\mu\mathrm{mol}\,\mathrm{m}^{-2}\,\mathrm{s}^{-1})$ for 0 or 8 or 12 or 24 h. Total protein was extracted and treated as described previously (Xu et al. 2021), and the endogenous HY5 and HY5-GFP fusion protein were analyzed by Western blotting with the antibodies against HY5 (Liu et al. 2022) and GFP, respectively.

Assays for protein localization and co-localization to the autophagosome and vacuole

WT, atg5 atg7, cry1, CRY1pro:CRY1/cry1, and CRY1pro:CRY1^{mAIM1}/ cry1 seedlings grown in darkness for 4 d, hypocotyls were cut off and submerged into the enzyme solution (1% cellulase R-10, 0.25% macerozyme R-10, 0.035% PectolyaseY-23, 0.4 M mannitol, 20 mm KCl, 20 mm MES, 0.5%BSA, 10 mm CaCl₂, pH 5.7), incubated in the dark overnight at 23 °C. After digestion, the mixture was filtered with $70 \, \mu m$ cell strainer (Falcon REF352340, Corning, Deeside, UK) and added the same volume of W5 solution (2 mm MES, 154 mm NaCl, 125 mm CaCl₂, 5 mm KCl), then centrifuge at 100 q for 3 min. Carefully remove all supernatants. The precipitation was resuspended with 10 mL W5 solution and placed on ice for 30 min away from light. Finally, centrifuged to remove the supernatant and then resuspended with an appropriate amount of MMG (4 mm MES, 0.4 mm mannitol, 15 mm MgCl₂). The cassettes harboring 35S:HY5-GFP, 35S:HY5-mCherry, 35S:mCherry-ATG8a, 35S:mCherry-ATG8e, and 35S:H3-YFP were constructed in pA7 vector (Xu et al. 2018). Hypocotyl protoplasts were transfected with different combinations of constructs and incubated in W5-C-N solution in darkness for 7 or 16 h, and then transferred into W5 +C+N (1% sucrose, 20.6 mm NH₄NO₃, and 18.8 mm KNO₃) and/or W5-C-N solution supplemented with ConA (1 μ M) and with or without CHX (50 μ M) (MCE) and adapted in darkness and/or exposed to blue light for 24 h before subjected to confocal microscopy. GFP, YFP, and mCherry were excited using 489 nm (40% to 100% intensity, gain: 100 to 250 V), 514 nm (10% intensity,

gain: 30 to 100 V) and 587 nm (40% to 60% intensity, gain: 60 to 140 V) lasers with emission signals collected at 495 to 530 nm (GFP), 520 to 540 nm (YFP) and 590 to 630 nm (mCherry), respectively.

Protein localization assay for YFP-ATG8

YFP-8a-i-OX seedlings were grown in white light for 5 d before their roots were detected by confocal microscopy. YFP and DAPI were excited using 514 nm (10% to 20% intensity, gain: 80 to 240 V) and 405 nm (30% intensity, gain: 80 V) with emission signals collected at 519 to 590 and 433 to 475 nm, respectively.

Nuclear and cytoplasmic protein separation assays

YFP-8e-OX and YFP-8e-OX/cry1 were grown in white (100 μ mol m⁻² s⁻¹) for 4 d, and then transferred to liquid MS+C+N and/or MS-C-N medium supplemented with or without CHX (100 μ M) and adapted in darkness or exposed to blue light (90 μ mol m⁻² s⁻¹) for 12 h. Cytoplasmic and nuclear fractions were prepared as described previously with minor modifications (Zhang et al. 2023; Zhao et al. 2023). Briefly, seedlings were homogenized with lysis buffer, and the homogenates were filtered through 2 layers of Miracloth. The flow-through was centrifuged at 1,500 q at 4 °C for 10 min. Then, the supernatant was taken as the cytosolic fraction. The nuclear pellet was washed twice with the nuclear resuspension buffer with and then without 0.5% NP40 sequentially. The supernatant (cytosolic fraction) and pellet (nuclear protein) were boiled in SDS-PAGE loading buffer and analyzed by Western blotting. UGPase and H3 served as cytoplasmic and nuclear fraction markers, respectively.

GFP-ATG8-labeled autophagosome production observation

YFP-8a-OX, YFP-8e-OX, YFP-8e-OX/atq5 atq7, YFP-8a-OX/cry1, and YFP-8e-OX/cry1 seedlings were grown on MS+C+N medium in white light (100 μ mol m⁻² s⁻¹) 4 d, and then transferred into liquid MS-C-N medium supplemented with CHX (100 μ M) and with or without ConA (1 μ M). Then adapted in darkness or exposed to blue light (90 μ mol m⁻² s⁻¹) for 8 h. The autophagosomes produced in the roots of the indicated genotypes of seedlings were analyzed by confocal microscopy. YFP was excited using 514 nm (100% and 10% to 20% intensity, gain: 80 to 240 V) with emission signals collected at 519 to 590 nm with or without CHX, respectively.

Accession numbers

Sequence data from this article can be found in the EMBL/GenBank database or the Arabidopsis Genome Initiative database under the following accession numbers: CRY1 (At4g08920), ATG8a (At4g21980), ATG8b (At4g04620), ATG8c (At1g62040), ATG8d (At2g05630), ATG8e (At2g45170), ATG8f (At4g16520), and ATG8g (At3g60640), ATG8h (At3g06420), ATG8i (At3g15580), ATG5 (At5g17290), ATG7 (At5g45900), ATG11 (At4g30790), HY5 (At5g11260).

Acknowledgments

We thank Drs. Jirong Huang, Jigang Li, and Haodong Chen for providing atg5/atg7 seeds, pLexA-JL vector, and CRISPR-Cas9 system, and Drs. Peng Zhang and Yaqi Liu for helpful discussion about the modeled structure of AtCRY1-PHR.

Author contributions

W.W. and H.-Q.Y. conceived the project; W.W., H.-Q.Y., L.J., and S.Z. designed the research plan; W.W., L.J., S.Z., G.Y., J.Z., H.L., M.X., Y.N., L.X., Z.M., and T.G. carried out the experiments; W.W., L.J., and S.Z. analyzed the data; W.W., L.J., S.Z., and H.-Q.Y. wrote the manuscript.

Supplementary data

The following materials are available in the online version of this article

Supplementary Figure S1. CNT1 interacts with ATG8 in yeast. **Supplementary Figure S2.** Mutating the AIM motif within CRY1 affects its interaction with ATG8.

Supplementary Figure S3. The AIM1 motif is essential for CRY1-mediated rescue of the *cry1* tall-hypocotyl phenotype.

Supplementary Figure S4. ATG5, ATG7, and ATG11 positively regulate hypocotyl elongation in low blue light conditions.

Supplementary Figure S5. Sequence confirmation of *atg8n*, *cry1 atg8n*, and *atg8n* hy5 decuple mutants generated by CRISPR-Cas9-mediated gene editing.

Supplementary Figure S6. HY5 is degraded in darkness through the autophagy pathway.

Supplementary Figure S7. ATG8 physically interacts with HY5 through its UDS motif.

Supplementary Figure S8. Blue light inhibits the co-localization of HY5-GFP and mCherry-ATG8e to the autophagosome.

Supplementary Figure S9. ATG8 proteins are localized in both the nucleus and cytoplasm.

Supplementary Figure S10. CRY1 inhibits ATG8 export from the nucleus, and ATG5 and ATG7 inhibit autophagosome formation in Arabidopsis.

Supplementary Figure S11. The structure of AtCRY1-PHR modeled according to ZmCRY1c.

Supplementary Figure S12. HY5-GFP is degraded faster under nutrient starvation during early skotomorphogenic development after seed germination in darkness.

Supplementary Data Set 1. Primers used in this study. **Supplementary Data Set 2.** Statistical analysis results.

Funding

This work was supported by the National Natural Science Foundation of China grant number (32370262), the National Key Research and Development Program of China grant (2024YFA1306702).

Conflict of interest statement. None declared.

Data availability

The data underlying this article cannot be shared publicly due to the privacy of individuals that participated in the study. The data will be shared on reasonable request to the corresponding author.

References

- Ahmad M, Cashmore AR. HY4 gene of A. thaliana encodes a protein with characteristics of a blue-light photoreceptor. Nature. 1993:366(6451):162–166. https://doi.org/10.1038/366162a0
- Alonso JM, Stepanova AN, Leisse TJ, Kim CJ, Chen H, Shinn P, Stevenson DK, Zimmerman J, Barajas P, Cheuk R, et al. Genome-wide insertional mutagenesis of Arabidopsis thaliana.

- Science. 2003:301(5633):653–657. https://doi.org/10.1126/science. 1086391
- Bao Y, Song WM, Wang P, Yu X, Li B, Jiang C, Shiu SH, Zhang H, Bassham DC. COST1 regulates autophagy to control plant drought tolerance. *Proc Natl Acad Sci U S A.* 2020:117(13): 7482–7493. https://doi.org/10.1073/pnas.1918539117
- Briggs WR, Christie JM. Phototropins 1 and 2: versatile plant bluelight receptors. Trends Plant Sci. 2002:7(5):204–210. https://doi. org/10.1016/S1360-1385(02)02245-8
- Bu F, Yang M, Guo X, Huang W, Chen L. Multiple functions of ATG8 family proteins in plant autophagy. Front Cell Dev Biol. 2020:8: 466. https://doi.org/10.3389/fcell.2020.00466
- Cao X, Xu P, Liu Y, Yang G, Liu M, Chen L, Cheng Y, Xu P, Miao L, Mao Z, et al. *Arabidopsis* cryptochrome 1 promotes stomatal development through repression of AGB1 inhibition of SPEECHLESS DNA-binding activity. *J Integr Plant Biol*. 2021:63(11):1967–1981. https://doi.org/10.1111/jipb.13168
- Chen X, Yao Q, Gao X, Jiang C, Harberd NP, Fu X. Shoot-to-root mobile transcription factor HY5 coordinates plant carbon and nitrogen acquisition. *Curr Biol.* 2016:26(5):640–646. https://doi.org/10.1016/j.cub.2015.12.066
- Chung T, Suttangkakul A, Vierstra RD. The ATG autophagic conjugation system in maize: ATG transcripts and abundance of the ATG8-lipid adduct are regulated by development and nutrient availability. Plant Physiol. 2009:149(1):220–234. https://doi.org/10.1104/pp.108.126714
- Deng XW, Matsui M, Wei N, Wagner D, Chu AM, Feldmann KA, Quail PH. COP1, an *Arabidopsis* regulatory gene, encodes a protein with both a zinc-binding motif and a G beta homologous domain. *Cell*. 1992:71(5):791–801. https://doi.org/10.1016/0092-8674(92)90555-Q
- Deng XW, Quail PH. Signalling in light-controlled development. Semin Cell Dev Biol. 1999:10(2):121–129. https://doi.org/10.1006/scdb.1999.0287
- Doelling JH, Walker JM, Friedman EM, Thompson AR, Vierstra RD. The APG8/12-activating enzyme APG7 is required for proper nutrient recycling and senescence in *Arabidopsis thaliana*. *J Biol Chem.* 2002:277(36):33105–33114. https://doi.org/10.1074/jbc.M204630200
- Dou Z, Xu C, Donahue G, Shimi T, Pan J-A, Zhu J, Ivanov A, Capell BC, Drake AM, Shah PP, et al. Autophagy mediates degradation of nuclear lamina. *Nature*. 2015:527(7576):105–109. https://doi.org/10.1038/nature15548
- Du SS, Li L, Li L, Wei X, Xu F, Xu P, Wang W, Xu P, Cao X, Miao L, et al. Photoexcited cryptochrome2 interacts directly with TOE1 and TOE2 in flowering regulation. Plant Physiol. 2020:184(1):487–505. https://doi.org/10.1104/pp.20.00486
- Emery P, So WV, Kaneko M, Hall JC, Rosbash M. CRY, a Drosophila clock and light-regulated cryptochrome, is a major contributor to circadian rhythm resetting and photosensitivity. Cell. 1998:95(5): 669–679. https://doi.org/10.1016/S0092-8674(00)81637-2
- Favory JJ, Stec A, Gruber H, Rizzini L, Oravecz A, Funk M, Albert A, Cloix C, Jenkins GI, Oakeley EJ, et al. Interaction of COP1 and UVR8 regulates UV-B-induced photomorphogenesis and stress acclimation in Arabidopsis. Embo J. 2009:28(5):591–601. https:// doi.org/10.1038/emboj.2009.4
- Gao J, Wang X, Zhang M, Bian M, Deng W, Zuo Z, Yang Z, Zhong D, Lin C. Trp triad-dependent rapid photoreduction is not required for the function of Arabidopsis CRY1. Proc Natl Acad Sci U S A. 2015:112(29):9135–9140. https://doi.org/10.1073/pnas.1504404112
- Gegear RJ, Foley LE, Casselman A, Reppert SM. Animal cryptochromes mediate magnetoreception by an unconventional photochemical mechanism. Nature. 2010:463(7282):804–807. https:// doi.org/10.1038/nature08719

- Guo H, Yang H, Mockler TC, Lin C. Regulation of flowering time by Arabidopsis photoreceptors. Science. 1998:279(5355):1360–1363. https://doi.org/10.1126/science.279.5355.1360
- Guo T, Liu M, Chen L, Liu Y, Li L, Li Y, Cao X, Mao Z, Wang W, Yang HQ. Photoexcited cryptochromes interact with ADA2b and SMC5 to promote the repair of DNA double-strand breaks in Arabidopsis. Nat Plants. 2023:9(8):1280–1290. https://doi.org/10.1038/s41477-023-01461-6
- Hanada T, Noda NN, Satomi Y, Ichimura Y, Fujioka Y, Takao T, Inagaki F, Ohsumi Y. The Atg12-Atg5 conjugate has a novel E3-like activity for protein lipidation in autophagy. *J Biol Chem.* 2007:282(52): 37298–37302. https://doi.org/10.1074/jbc.C700195200
- Hardtke CS, Gohda K, Osterlund MT, Oyama T, Okada K, Deng XW. HY5 stability and activity in Arabidopsis is regulated by phosphorylation in its COP1 binding domain. EMBO J. 2000:19(18): 4997–5006. https://doi.org/10.1093/emboj/19.18.4997
- Hoecker U, Tepperman JM, Quail PH. SPA1, a WD-repeat protein specific to phytochrome A signal transduction. *Science*. 1999:284(5413): 496–499. https://doi.org/10.1126/science.284.5413.496
- Hu Z, Yang Z, Zhang Y, Zhang A, Lu Q, Fang Y, Lu C. Autophagy targets Hd1 for vacuolar degradation to regulate rice flowering. Mol Plant. 2022:15(7):1137–1156. https://doi.org/10.1016/j.molp.2022.05.006
- Huang F, Luo X, Ou Y, Gao Z, Tang Q, Chu Z, Zhu X, He Y. Control of histone demethylation by nuclear-localized alpha-ketoglutarate dehydrogenase. Science. 2023:381(6654):eadf8822. doi:10.1126/ science.adf8822
- Huang X, Zheng C, Liu F, Yang C, Zheng P, Lu X, Tian J, Chung T, Otegui MS, Xiao S, et al. Genetic analyses of the Arabidopsis ATG1 kinase complex reveal both kinase-dependent and independent autophagic routes during fixed-carbon starvation. Plant Cell. 2019:31(12):2973–2995. https://doi.org/10.1105/tpc.19.00066
- Ince YC, Krahmer J, Fiorucci AS, Trevisan M, Galvao VC, Wigger L, Pradervand S, Fouillen L, Van Delft P, Genva M, et al. A combination of plasma membrane sterol biosynthesis and autophagy is required for shade-induced hypocotyl elongation. *Nat Commun.* 2022:13(1):5659. https://doi.org/10.1038/s41467-022-33384-9
- Jang IC, Henriques R, Seo HS, Nagatani A, Chua NH. Arabidopsis PHYTOCHROME INTERACTING FACTOR proteins promote phytochrome B polyubiquitination by COP1 E3 ligase in the nucleus. Plant Cell. 2010:22(7):2370–2383. https://doi.org/10.1105/tpc.109.072520
- Jia KP, Luo Q, He SB, Lu XD, Yang HQ. Strigolactone-regulated hypocotyl elongation is dependent on cryptochrome and phytochrome signaling pathways in Arabidopsis. Mol Plant. 2014:7(3): 528–540. https://doi.org/10.1093/mp/sst093
- Johansen T, Lamark T. Selective autophagy: ATG8 family proteins, LIR motifs and cargo receptors. J Mol Biol. 2020:432(1):80–103. https://doi.org/10.1016/j.jmb.2019.07.016
- Kang CY, Lian HL, Wang FF, Huang JR, Yang HQ. Cryptochromes, phytochromes, and COP1 regulate light-controlled stomatal development in Arabidopsis. Plant Cell. 2009:21(9):2624–2641. https://doi.org/10.1105/tpc.109.069765
- Kume K, Zylka MJ, Sriram S, Shearman LP, Weaver DR, Jin X, Maywood ES, Hastings MH, Reppert SM. mCRY1 and mCRY2 are essential components of the negative limb of the circadian clock feedback loop. Cell. 1999:98(2):193–205. https://doi.org/10.1016/ S0092-8674(00)81014-4
- Lai Z, Wang F, Zheng Z, Fan B, Chen Z. A critical role of autophagy in plant resistance to necrotrophic fungal pathogens. *Plant J.* 2011:66(6): 953–968. https://doi.org/10.1111/j.1365-313X.2011.04553.x

- Lamark T, Johansen T. Mechanisms of selective autophagy. Annu Rev Cell Dev Biol. 2021:37(1):143–169. https://doi.org/10.1146/annurevcellbio-120219-035530
- Li H, Qin X, Song P, Han R, Li J. A LexA-based yeast two-hybrid system for studying light-switchable interactions of phytochromes with their interacting partners. aBIOTECH. 2021:2(2):105–116. https://doi.org/10.1007/s42994-021-00034-5
- Lian H, Xu P, He S, Wu J, Pan J, Wang W, Xu F, Wang S, Pan J, Huang J, et al. Photoexcited CRYPTOCHROME 1 interacts directly with G-protein beta subunit AGB1 to regulate the DNA-binding activity of HY5 and photomorphogenesis in *Arabidopsis*. Mol Plant. 2018:11(10):1248–1263. https://doi.org/10.1016/j.molp. 2018.08.004
- Lian HL, He SB, Zhang YC, Zhu DM, Zhang JY, Jia KP, Sun SX, Li L, Yang HQ. Blue-light-dependent interaction of cryptochrome 1 with SPA1 defines a dynamic signaling mechanism. *Genes Dev.* 2011:25(10):1023–1028. https://doi.org/10.1101/gad.2025111
- Liu B, Zuo Z, Liu H, Liu X, Lin C. Arabidopsis cryptochrome 1 interacts with SPA1 to suppress COP1 activity in response to blue light. Genes Dev. 2011:25(10):1029–1034. https://doi.org/10.1101/gad. 2025011
- Liu F, Hu W, Li F, Marshall RS, Zarza X, Munnik T, Vierstra RD. AUTOPHAGY-RELATED14 and its associated phosphatidylinositol 3-kinase complex promote autophagy in *Arabidopsis*. *Plant Cell*. 2020:32(12):3939–3960. https://doi.org/10.1105/tpc.20.00285
- Liu LJ, Zhang YC, Li QH, Sang Y, Mao J, Lian HL, Wang L, Yang HQ. COP1-mediated ubiquitination of CONSTANS is implicated in cryptochrome regulation of flowering in Arabidopsis. Plant Cell. 2008;20(2):292–306. https://doi.org/10.1105/tpc.107.057281
- Liu S, Zhang L, Gao L, Chen Z, Bie Y, Zhao Q, Zhang S, Hu X, Liu Q, Wang X, et al. Differential photoregulation of the nuclear and cytoplasmic CRY1 in Arabidopsis. New Phytol. 2022:234(4):1332–1346. https://doi.org/10.1111/nph.18007
- Ma D, Li X, Guo Y, Chu J, Fang S, Yan C, Noel JP, Liu H. Cryptochrome 1 interacts with PIF4 to regulate high temperature-mediated hypocotyl elongation in response to blue light. Proc Natl Acad Sci U S A. 2016:113(1):224–229. https://doi.org/10.1073/pnas.1511437113
- Ma L, Li X, Zhao Z, Hao Y, Shang R, Zeng D, Liu H. Light-response Bric-A-Brack/Tramtrack/Broad proteins mediate cryptochrome 2 degradation in response to low ambient temperature. Plant Cell. 2021:33(12):3610–3620. https://doi.org/10.1093/ plcell/koab219
- Mao J, Zhang YC, Sang Y, Li QH, Yang HQ. From the cover: a role for Arabidopsis cryptochromes and COP1 in the regulation of stomatal opening. Proc Natl Acad Sci U S A. 2005:102(34):12270–12275. https://doi.org/10.1073/pnas.0501011102
- Mao Z, He S, Xu F, Wei X, Jiang L, Liu Y, Wang W, Li T, Xu P, Du S, et al. Photoexcited CRY1 and phyB interact directly with ARF6 and ARF8 to regulate their DNA-binding activity and auxin-induced hypocotyl elongation in *Arabidopsis*. *New Phytol*. 2020:225(2): 848–865. https://doi.org/10.1111/nph.16194
- Mao Z, Wei X, Li L, Xu P, Zhang J, Wang W, Guo T, Kou S, Wang W, Miao L, et al. Arabidopsis cryptochrome 1 controls photomorphogenesis through regulation of H2A.Z deposition. Plant Cell. 2021:33(6):1961–1979. https://doi.org/10.1093/plcell/koab091
- Marshall RS, Hua Z, Mali S, McLoughlin F, Vierstra RD. ATG8-Binding UIM proteins define a new class of autophagy adaptors and receptors. *Cell.* 2019:177(3):766–781.e724. https://doi.org/10.1016/j.cell. 2019.02.009
- Marshall RS, Li F, Gemperline DC, Book AJ, Vierstra RD. Autophagic degradation of the 26S proteasome is mediated by the dual ATG8/ubiquitin receptor RPN10 in Arabidopsis. Mol

- Cell. 2015:58(6):1053–1066. https://doi.org/10.1016/j.molcel.2015. 04.023
- Marshall RS, Vierstra RD. Autophagy: the master of bulk and selective recycling. Annu Rev Plant Biol. 2018:69(1):173–208. https://doi.org/10.1146/annurev-arplant-042817-040606
- Merkulova EA, Guiboileau A, Naya L, Masclaux-Daubresse C, Yoshimoto K. Assessment and optimization of autophagy monitoring methods in *Arabidopsis* roots indicate direct fusion of autophagosomes with vacuoles. *Plant Cell Physiol*. 2014:55(4):715–726. https://doi.org/10.1093/pcp/pcu041
- Miao L, Zhao J, Yang G, Xu P, Cao X, Du S, Xu F, Jiang L, Zhang S, Wei X, et al. Arabidopsis cryptochrome 1 undergoes COP1 and LRBs-dependent degradation in response to high blue light. New Phytol. 2022;234(4):1347–1362. https://doi.org/10.1111/nph.17695
- Minina EA, Moschou PN, Vetukuri RR, Sanchez-Vera V, Cardoso C, Liu Q, Elander PH, Dalman K, Beganovic M, Lindberg Yilmaz J, et al. Transcriptional stimulation of rate-limiting components of the autophagic pathway improves plant fitness. *J Exp Bot.* 2018:69(6):1415–1432. https://doi.org/10.1093/jxb/ery010
- Nakatogawa H. Two ubiquitin-like conjugation systems that mediate membrane formation during autophagy. Essays Biochem. 2013:55:39–50. https://doi.org/10.1042/bse0550039
- Nakatogawa H, Ichimura Y, Ohsumi Y. Atg8, a ubiquitin-like protein required for autophagosome formation, mediates membrane tethering and hemifusion. *Cell*. 2007:130(1):165–178. https://doi.org/10.1016/j.cell.2007.05.021
- Nolan TM, Brennan B, Yang MR, Chen JN, Zhang MC, Li ZH, Wang XL, Bassham DC, Walley J, Yin YH. Selective autophagy of BES1 mediated by DSK2 balances plant growth and survival. *Dev Cell*. 2017:41(1):33–46.e7. https://doi.org/10.1016/j.devcel.2017.03.013
- Ohgishi M, Saji K, Okada K, Sakai T. Functional analysis of each blue light receptor, cry1, cry2, phot1, and phot2, by using combinatorial multiple mutants in *Arabidopsis*. *Proc Natl Acad Sci U S A*. 2004:101(8):2223–2228. https://doi.org/10.1073/pnas.0305984101
- Ohsumi Y. Historical landmarks of autophagy research. Cell Res. 2014:24(1):9–23. https://doi.org/10.1038/cr.2013.169
- Osterlund MT, Hardtke CS, Wei N, Deng XW. Targeted destabilization of HY5 during light-regulated development of Arabidopsis. Nature. 2000:405(6785):462–466. https://doi.org/10.1038/35013076
- Oyama T, Shimura Y, Okada K. The Arabidopsis HY5 gene encodes a bZIP protein that regulates stimulus-induced development of root and hypocotyl. Genes Dev. 1997:11(22):2983–2995. https://doi.org/10.1101/gad.11.22.2983
- Pedmale UV, Huang SC, Zander M, Cole BJ, Hetzel J, Ljung K, Reis PAB, Sridevi P, Nito K, Nery JR, et al. Cryptochromes interact directly with PIFs to control plant growth in limiting blue light. *Cell*. 2016:164(1-2):233–245. https://doi.org/10.1016/j.cell.2015.12.018
- Qi H, Xia FN, Xiao S. Autophagy in plants: physiological roles and post-translational regulation. *J Integr Plant Biol.* 2021:63(1): 161–179. https://doi.org/10.1111/jipb.12941
- Qi H, Xia FN, Xie LJ, Yu LJ, Chen QF, Zhuang XH, Wang Q, Li F, Jiang L, Xie Q, et al. TRAF family proteins regulate autophagy dynamics by modulating AUTOPHAGY PROTEIN6 stability in Arabidopsis. Plant Cell. 2017:29(4):890–911. https://doi.org/10.1105/tpc.17.00056
- Qu GP, Jiang B, Lin C. The dual-action mechanism of Arabidopsis cryptochromes. J Integr Plant Biol. 2024:66(5):883–896. https://doi.org/10.1111/jipb.13578
- Quail PH. Phytochrome photosensory signalling networks. Nat Rev Mol Cell Biol. 2002;3(2):85–93. https://doi.org/10.1038/nrm728
- Rizzini L, Favory JJ, Cloix C, Faggionato D, O'Hara A, Kaiserli E, Baumeister R, Schafer E, Nagy F, Jenkins GI, et al. Perception of UV-B by the Arabidopsis UVR8 protein. Science. 2011:332(6025): 103–106. https://doi.org/10.1126/science.1200660

- Romanov J, Walczak M, Ibiricu I, Schüchner S, Ogris E, Kraft C, Martens S. Mechanism and functions of membrane binding by the Atg5-Atg12/Atg16 complex during autophagosome formation. EMBO J. 2012:31(22):4304–4317. https://doi.org/10.1038/emboj.2012.278
- Sang Y, Li QH, Rubio V, Zhang YC, Mao J, Deng XW, Yang HQ. N-terminal domain-mediated homodimerization is required for photoreceptor activity of Arabidopsis CRYPTOCHROME 1. Plant Cell. 2005:17(5):1569–1584. https://doi.org/10.1105/tpc.104.029645
- Seo HS, Watanabe E, Tokutomi S, Nagatani A, Chua NH. Photoreceptor ubiquitination by COP1 E3 ligase desensitizes phytochrome A signaling. *Genes Dev.* 2004:18(6):617–622. https://doi.org/10.1101/gad.1187804
- Seo HS, Yang JY, Ishikawa M, Bolle C, Ballesteros ML, Chua NH. LAF1 ubiquitination by COP1 controls photomorphogenesis and is stimulated by SPA1. *Nature*. 2003:423(6943):995–999. https://doi.org/10.1038/nature01696
- Shao K, Zhang X, Li X, Hao Y, Huang X, Ma M, Zhang M, Yu F, Liu H, Zhang P. The oligomeric structures of plant cryptochromes. *Nat* Struct Mol Biol. 2020:27(5):480–488. https://doi.org/10.1038/s41594-020-0420-x
- Somers DE, Devlin PF, Kay SA. Phytochromes and cryptochromes in the entrainment of the Arabidopsis circadian clock. Science. 1998:282(5393):1488–1490. https://doi.org/10.1126/science.282.5393.1488
- Taherbhoy AM, Tait SW, Kaiser SE, Williams AH, Deng A, Nourse A, Hammel M, Kurinov I, Rock CO, Green DR, et al. Atg8 transfer from Atg7 to Atg3: a distinctive E1-E2 architecture and mechanism in the autophagy pathway. Mol Cell. 2011:44(3):451–461. https://doi.org/10.1016/j.molcel.2011.08.034
- Thompson AR, Doelling JH, Suttangkakul A, Vierstra RD. Autophagic nutrient recycling in *Arabidopsis* directed by the ATG8 and ATG12 conjugation pathways. *Plant Physiol*. 2005:138(4):2097–2110. https://doi.org/10.1104/pp.105.060673
- Toledo M, Batista-Gonzalez A, Merheb E, Aoun ML, Tarabra E, Feng D, Sarparanta J, Merlo P, Botre F, Schwartz GJ, et al. Autophagy regulates the liver clock and glucose metabolism by degrading CRY1. Cell Metab. 2018:28(2):268–281 e264. https://doi.org/10.1016/j.cmet.2018.05.023
- Wang H, Ma LG, Li JM, Zhao HY, Deng XW. Direct interaction of Arabidopsis cryptochromes with COP1 in light control development. Science. 2001:294(5540):154–158. https://doi.org/10.1126/ science.1063630
- Wang JJ, Chen HD. A novel CRISPR/Cas9 system for efficiently generating Cas9-free multiplex mutants in. Abiotech. 2020:1(1):6–14. https://doi.org/10.1007/s42994-019-00011-z
- Wang P, Nolan TM, Clark NM, Jiang H, Montes-Serey C, Guo HQ, Bassham DC, Walley JW, Yin YH. The F-box E3 ubiquitin ligase BAF1 mediates the degradation of the brassinosteroid-activated transcription factor BES1 through selective autophagy in Arabidopsis. Plant Cell. 2021a:33(11):3532–3554. https://doi.org/10.1093/plcell/koab210
- Wang Q, Lin C. Mechanisms of cryptochrome-mediated photoresponses in plants. *Annu Rev Plant Biol*. 2020:71(1):103–129. https://doi.org/10.1146/annurev-arplant-050718-100300
- Wang Q, Zuo Z, Wang X, Gu L, Yoshizumi T, Yang Z, Yang L, Liu Q, Liu W, Han YJ, et al. Photoactivation and inactivation of *Arabidopsis* cryptochrome 2. Science. 2016:354(6310):343–347. https://doi.org/10.1126/science.aaf9030
- Wang W, Lu X, Li L, Lian H, Mao Z, Xu P, Guo T, Xu F, Du S, Cao X, et al.
 Photoexcited CRYPTOCHROME1 interacts with dephosphory-lated BES1 to regulate brassinosteroid signaling and

- photomorphogenesis in Arabidopsis. Plant Cell. 2018:30(9): 1989–2005. https://doi.org/10.1105/tpc.17.00994
- Wang X, Jiang B, Gu L, Chen Y, Mora M, Zhu M, Noory E, Wang Q, Lin C. A photoregulatory mechanism of the circadian clock in Arabidopsis. Nat Plants. 2021b:7(10):1397–1408. https://doi.org/10.1038/s41477-021-01002-z
- Wang X, Lin C. The two action mechanisms of plant cryptochromes. Trends Plant Sci. 2025:30(7):775–791. https://doi.org/10.1016/j. tplants.2024.12.001
- Wu G, Spalding EP. Separate functions for nuclear and cytoplasmic cryptochrome 1 during photomorphogenesis of Arabidopsis seed-lings. Proc Natl Acad Sci U S A. 2007:104(47):18813–18818. https://doi.org/10.1073/pnas.0705082104
- Xu C, Wang L, Fozouni P, Evjen G, Chandra V, Jiang J, Lu C, Nicastri M, Bretz C, Winkler JD, et al. SIRT1 is downregulated by autophagy in senescence and ageing. Nat Cell Biol. 2020:22(10):1170–1179. https://doi.org/10.1038/s41556-020-00579-5
- Xu F, He S, Zhang J, Mao Z, Wang W, Li T, Hua J, Du S, Xu P, Li L, et al. Photoactivated CRY1 and phyB interact directly with AUX/IAA proteins to inhibit auxin signaling in Arabidopsis. Mol Plant. 2018:11(4):523–541. https://doi.org/10.1016/j.molp.2017.12.003
- Xu P, Chen H, Li T, Xu F, Mao Z, Cao X, Miao L, Du S, Hua J, Zhao J, et al. Blue light-dependent interactions of CRY1 with GID1 and DELLA proteins regulate gibberellin signaling and photomorphogenesis in Arabidopsis. Plant Cell. 2021:33(7):2375–2394. https://doi.org/10.1093/plcell/koab124
- Yang C, Shen W, Yang L, Sun Y, Li X, Lai M, Wei J, Wang C, Xu Y, Li F, et al. HY5-HDA9 Module transcriptionally regulates plant autophagy in response to light-to-dark conversion and nitrogen starvation. Mol Plant. 2020:13(3):515–531. https://doi.org/10.1016/j.molp.2020.02.011
- Yang HQ, Tang RH, Cashmore AR. The signaling mechanism of Arabidopsis CRY1 involves direct interaction with COP1. Plant Cell. 2001:13(12):2573–2587. https://doi.org/10.1105/tpc.010367
- Yang HQ, Wu YJ, Tang RH, Liu D, Liu Y, Cashmore AR. The C termini of Arabidopsis cryptochromes mediate a constitutive light response. Cell. 2000:103(5):815–827. https://doi.org/10.1016/S0092-8674(00)00184-7

- Yoshimoto K, Hanaoka H, Sato S, Kato T, Tabata S, Noda T, Ohsumi Y. Processing of ATG8s, ubiquitin-like proteins, and their deconjugation by ATG4s are essential for plant autophagy. Plant Cell. 2004:16(11):2967–2983. https://doi.org/10.1105/tpc.104.025395
- Young PG, Passalacqua MJ, Chappell K, Llinas RJ, Bartel B. A facile forward-genetic screen for Arabidopsis autophagy mutants reveals twenty-one loss-of-function mutations disrupting six ATG genes. Autophagy. 2019:15(6):941–959. https://doi.org/10.1080/ 15548627.2019.1569915
- Yu X, Klejnot J, Zhao X, Shalitin D, Maymon M, Yang H, Lee J, Liu X, Lopez J, Lin C. Arabidopsis cryptochrome 2 completes its post-translational life cycle in the nucleus. Plant Cell. 2007:19(10): 3146–3156. https://doi.org/10.1105/tpc.107.053017
- Yu X, Liu H, Klejnot J, Lin C. The cryptochrome blue light receptors. *Arabidopsis Book.* 2010:8:e0135. https://doi.org/10.1199/tab.0135
- Zeng D, Lv J, Li X, Liu H. The Arabidopsis blue-light photoreceptor CRY2 is active in darkness to inhibit root growth. *Cell*. 2025:188(1):60–76.e20. https://doi.org/10.1016/j.cell.2024.10.031
- Zhan N, Wang C, Chen L, Yang H, Feng J, Gong X, Ren B, Wu R, Mu J, Li Y, et al. S-Nitrosylation targets GSNO reductase for selective autophagy during hypoxia responses in plants. *Mol Cell*. 2018:71(1): 142–154.e146. https://doi.org/10.1016/j.molcel.2018.05.024
- Zhang Q, Lin L, Fang F, Cui B, Zhu C, Luo S, Yin R. Dissecting the functions of COP1 in the UVR8 pathway with a COP1 variant in Arabidopsis. Plant J. 2023:113(3):478–492. https://doi.org/10.1111/tpj.16059
- Zhao Y, Shi H, Pan Y, Lyu M, Yang Z, Kou X, Deng XW, Zhong S. Sensory circuitry controls cytosolic calcium-mediated phytochrome B phototransduction. *Cell.* 2023:186(6):1230–1243.e1214. https://doi.org/10.1016/j.cell.2023.02.011
- Zhong M, Zeng B, Tang D, Yang J, Qu L, Yan J, Wang X, Li X, Liu X, Zhao X. The blue light receptor CRY1 interacts with GID1 and DELLA proteins to repress GA signaling during photomorphogenesis in Arabidopsis. Mol Plant. 2021:14(8):1328–1342. https://doi.org/10.1016/j.molp.2021.05.011